EVALUATION OF THE IMPACT OF AN ADDITIVE MANUFACTURING ENHANCED CUBESAT ARCHITECTURE ON THE CUBESAT DEVELOPMENT PROCESS

THESIS

Rachel E. Sharples

AFIT-ENV-MS-16-S-049

DEPARTMENT OF THE AIR FORCE
AIR UNIVERSITY

AIR FORCE INSTITUTE OF TECHNOLOGY

Wright-Patterson Air Force Base, Ohio

AFIT-ENV-MS-16-S-049

EVALUATION OF THE IMPACT OF AN ADDITIVE MANUFACTURING ENHANCED CUBESAT ARCHITECTURE ON THE CUBESAT DEVELOPMENT PROCESS

THESIS

Presented to the Faculty

Department of Systems Engineering and Management

Graduate School of Engineering and Management

Air Force Institute of Technology

Air University

Air Education and Training Command

In Partial Fulfillment of the Requirements for the

Degree of Master of Science in Systems Engineering

Rachel E. Sharples, Civilian, Ctr.

September 2016

AFIT-ENV-MS-16-S-049

EVALUATION OF THE IMPACT OF AN ADDITIVE MANUFACTURING ENHANCED CUBESAT ARCHITECTURE ON THE CUBESAT DEVELOPMENT PROCESS

Rachel E. Sharples, Civilian, Ctr.

Committee Membership:

Lt Col Jeffrey C. Parr, PhD
Chair

Dr. David Jacques
Member

Dr. Leslie Vaughn
Member

Abstract

Additive manufacturing (AM) is a fabrication method ideally suited to low-quantity, highly customized builds, leading to interest in the application of AM techniques to satellite development and manufacturing, where each build is unique. Due to the issues of long development schedules and high development and manufacturing costs, methods are needed in the CubeSat development process to reduce the weight and volume of subsystems and decrease integration time. The work develops an architecture for an AM-augmented CubeSat and examines how the AM techniques of embedded electronics, embedded thrusters, and custom radiation-hardened materials can impact the subsystems of a CubeSat. The AM-augmented architecture shows a shift in CubeSat development and manufacturing from a modular approach to an integrated approach where most of the CubeSat's internal bus components, such as electronics, thrusters, and propulsion, are integrated directly into the structure. This integrated approach results in decreased time spent in assembly and integration, decreased mass and volume, and also allows for key components to be embedded in materials with improved radiation attenuation characteristics. The end result of the architecture is a quantitative demonstration of how AM techniques can decrease mass, decrease volume, increase delta V (a measure of the impulse necessary to perform a maneuver in m/s), and increase radiation attenuation up to twice that of standard aluminum panels while also decreasing the mass of the structure itself by 22%.

Acknowledgments

I would like to thank my thesis advisor, Lt Col Jeff Parr, for his guidance and support throughout the course of this thesis effort. I would also like to thank my other committee members, Dr. David Jacques and Dr. Leslie Vaughn, for their insight and expertise. Many thanks to my family and friends for their support not only through this thesis effort but also through the preceding years of coursework.

Rachel E. Sharples

Table of Contents

Page

List of Figures

Page

List of Tables

Page

List of Acronyms and Definitions

1U	10 cm x 10 cm x 10cm, unit volume size for CubeSats
3D	Three-Dimensional
ABS	Acrylonitrile Butadiene Styrene
ABS-M20	A type of ABS thermoplastic
ADACS	Attitude Determination and Control System
AM	Additive Manufacturing
AV-1	Overview and Summary Information
CAD	Computer-Aided Design
C-Class	Communications-Class
DP	Direct Print
DW	Direct Write
E-Class	Education-Class
ELaNa	Educational Launch of Nanosatellites
FST	Flame, Smoke, and Toxicity
GPS	Global Positioning System
OV-5a	Operational Activity Model
PC	Polycarbonate
PC-ABS	PC and ABS thermoplastic
PCB	Printed Circuit Board
PIC	Programmable Intelligent Computer
RAMPART	RApidprototyped MEMS Propulsion and Radiation Test
RF	Radio Frequency
S-Class	Science-Class
SLA	Stereolithography
SLS	Selective Laser Sintering
STL	STereoLithography (file format)
SV-1	Systems Interface Description
SV-4	Systems Functionality Description
SvcV-1	Services Context Description
SvcV-3a	Systems-Services Matrix
SvcV-5	Operational Activities to Services Traceability Matrix
SvcV-7	Services-Measures Matrix
SWaP	Size, Weight, and Power
T-Class	Technology-Class
TNC	Trajectory, Navigation, and Control
TT&C	Telemetry, Tracking, and Command
ULTEM	A type of polyetherimide thermoplastic

EVALUATION OF THE IMPACT OF AN ADDITIVE MANUFACTURING ENHANCED CUBESAT ARCHITECTURE ON THE CUBESAT DEVELOPMENT PROCESS

I. Introduction

Background or General Issue

Additive manufacturing (AM), also known as three-dimensional (3D) printing, is a manufacturing method where components are built up by adding successive layers of material, compared to more traditional manufacturing methods which are subtractive in nature—material is removed to create the desired geometry. Unlike some other traditional manufacturing methods, there is little to no upfront tooling costs, making AM ideal for low-volume applications, such as rapid prototyping, which uses AM's ability to adapt to changes in design and quickly produce a part with the geometry of the end design. For these same reasons, however, until relatively recently, rapid prototyping for development of a design prior to mass production has been the main commercial application of AM technology. The advent of 3D printing in materials other than plastic has led to an interest in applications of AM as a manufacturing method of end products in situations where a large production volume is not required and where the flexible nature of AM can actually be an improvement over traditional manufacturing techniques.

One area of recent interest is the application of AM to satellite development and manufacturing. Due to the fledgling nature of the technology, CubeSats, small, low-cost satellites, are an excellent vehicle for the exploration of applications of AM techniques in the space environment. The low cost and small size of CubeSats make them ideal for

university satellite build teams and other proof-of-concept research experiments. CubeSats are usually measured in units of "U", where 1U is a 10 cm edge cube; examples of standard sizes are 1U, 2U, 3U, 6U, 12U, and even up to 24U. CubeSats usually launch as secondary payloads and have specially built pods to allow them to easily interface with a launch vehicle.

Since each satellite is unique, mass production methods offer no advantage. Because AM techniques would increase the ease and speed of customization without high investment in non-recurring processes, they have the potential to enable spacecraft designs to be readily adapted to diverse customer needs without substantial development costs. Areas of proposed benefit include reducing size, weight, and power (SWaP) by embedding electronics and sensors directly into the spacecraft structure, enabling previously impossible propulsion designs by using AM's ability to create unique geometries that are not achievable with traditional manufacturing techniques; and building radiation protection directly into the spacecraft structures by developing radiation-hardened printable materials.

From a system perspective, if these proposed benefits are realizable, it would be possible to print key portions of the satellite with all of the electronics and sensors embedded in radiation hardened material and an integrated propulsion system that is part of the satellite itself, all at a smaller volume. Because these elements are already printed as a single item, fabricating a satellite in this manner would decrease the amount of integration required and thus decrease development time. If these portions of the satellite-printing process itself were to become space qualified, then a CubeSat made with this AM-augmented architecture would require very little time in the integration and

testing phase, allowing the CubeSat developer to focus resources on the experiment to be performed rather than on re-inventing the CubeSat for each new launch.

Problem Statement

To address the issues of long development schedules and high development and manufacturing costs, methods are needed in the CubeSat development process to reduce the weight and volume of subsystems and decrease integration time.

Research Objective and Investigative Questions

This research will quantitatively address the impact of proposed benefits of a 3D printed satellite architecture on the subsystems of a CubeSat. The objective of this research is to bring a quantitative analysis to the discussion of whether a fully 3D printed satellite architecture has a significant enough impact on a CubeSat launch to warrant investment.

The research will focus on the following three investigative questions:

1. What would a 3D printed CubeSat architecture look like?
2. On what CubeSat subsystem, if any, would a 3D printed CubeSat architecture have the greatest impact?
3. Which of the proposed benefits of 3D printing, such as optimization of mass and volume using embedded electronics, the ability to produce unusual geometries for unique propulsion and attitude control systems, and increased radiation protection from embedding components in custom materials, would have the greatest impact on the development of a CubeSat?

Methodology

The methodology will consist of developing an architecture and analyzing that architecture with respect to the systems and processes involved in a CubeSat launch. It will be assumed that the technology to print key components of a CubeSat exists; based on this assumption, an architecture for a printed CubeSat launch will be developed in Enterprise Architect. Because the purpose of this research is to examine the value of this potential system, the architecture will be detailed enough for evaluation only. Based on this architecture, quantitative risk models will be developed in Risk Solver Platform for Excel to determine the impact of the previously identified potential benefits of 3D printing technology on the phases of a CubeSat launch, and the results of these models will provide discussion as to whether a fully printed CubeSat provides enough benefit to merit investment.

Assumptions and Limitations

This work assumes that the technology already exists to manufacture key components of a satellite with additive manufacturing. Research into the viability of printing various subsystems is already underway, although the process for printing an entire satellite is still a ways from reality. One of the driving goals of this work is to begin to examine whether the proposed benefits of this technology would in fact be sufficient to be worth the investment to take the technology from its current university-level research stage to a process capable of producing integrated flight hardware. However, actually determining whether the technology warrants Air Force investment is outside the scope of this work. The hope is that the results of this research will feed into

such a discussion that will provide a worthwhile path forward for the application of AM technology.

Expected Contributions

Proponents of additive manufacturing propose many potential benefits of this technology for space applications. The three main areas identified for study in this work are embedding electronics and other components to optimize mass and volume using embedded electronics, enabling the production of propulsion and attitude control systems that rely on AM's ability to produce unique geometries, and embedding components in custom materials to increase radiation protection. This work will provide a quantitative analysis of the actual impact of some of these proposed benefits throughout the CubeSat development and life cycles, which will feed into the discussion of whether or not additive manufacturing technology for satellites is worth Air Force investment.

Preview

The literature review in Chapter 2 defines the subsystems and development cycle of a CubeSat, reviews prior research on 3D printed satellite subsystems, and identifies embedded electronics, thrusters, and radiation hardening through AM materials as three main proposed benefits of AM-augmented CubeSats. The methodology in Chapter 3 provides the overview and summary information (AV-1) of an AM-augmented CubeSat architecture and describes how the architecture will be quantitatively evaluated against selected measures. In addition, quantitative statistical predictive models based on CubeSat kit and component manufacturers' data are developed and presented in the methodology. The analysis and results in Chapter 4 present the AM-augmented

architecture views outlined in the AV-1, compares the systems definition and functional allocation to a baseline CubeSat architecture to identify the shift from a modular to an integrated architecture, and maps AM techniques to proposed benefits, subsystems, and measures. Chapter 4 also takes a qualitative look at how AM impacts the assembly, integration, and test schedule, and presents results of the predictive models developed in Chapter 3. Finally, the conclusions and recommendations in Chapter 5 summarizes the work, answers the three investigative questions presented in this chapter, provides recommendations for future work, and addresses the overall impact of this study.

II. Literature Review

Chapter Overview

The purpose of this chapter is to define the subsystems and development cycle of a CubeSat, and to identify previous research on 3D printed satellites and satellite subsystems. The AM research discussed in this literature review will lead to the identification of the three main proposed benefits that will be examined with respect to the CubeSat development subsystems as defined in this chapter, as well as the development of a simple printed satellite architecture for examination, during the methodology part of this work.

CubeSat Overview

The CubeSat architecture was first developed in 1999, and the first CubeSat was launched four years later in 2003 (Swartwout, 2013). The CubeSat's single most distinguishing feature is its compatibility with a standardized launch interface; the first such standardized interface was the Poly-PicoSatellite Orbital Deployer (P-POD), and there are a number of other CubeSat interfaces available today (Swartwout, 2013). The standardized launch interface was such a major development because it decouples the development of the launch interface from the development of the satellite (Swartwout, 2013). Similarly, a 3D-printed CubeSat architecture has the potential to decouple the development of the satellite from the integration and verification processes.

The unit (1U) size of a CubeSat is 10 cm x 10 cm x 11 cm; a 2U satellite would have the footprint of two 1U satellites stacked together, and so on. The majority of CubeSats developed and launched from the inception of the CubeSat through 2012 have

been 1U satellites, with the 3U satellite as the second most popular size (Swartwout, 2013). Launches can range from 1 to over 9 satellites per launch vehicle (Swartwout, 2013). CubeSats can be sorted into 4 classes: E-class, C-class, S-class, and T-class (Swartwout, 2013). E-class satellites are "education" satellites; their primary goal is to train students, and any actual mission objective is secondary to the students' hands-on experience with the satellite (Swartwout, 2013). C-class satellites are communications satellites with the goal of providing communication services (Swartwout, 2013). S-class satellites are "science" satellites and have a mission objective to collect data using methods such as remote sensing (Swartwout, 2013). T-class satellites are technology-class satellites that test technologies new to the industry (Swartwout, 2013). In 2012 there were more T-class CubeSat missions than any other class, followed by E-class (Swartwout, 2013). This prevalence of using CubeSat missions to test new technologies makes them an ideal vehicle to explore an additive manufacturing satellite architecture.

While initially used almost exclusively by universities, as the technology has matured the CubeSat form factor has been increasingly adopted in the industry, which has likely impacted the use of CubeSats for missions other than E-class (Swartwout, 2013). In addition, launch programs such as NASA's ELaNa (Educational Launch of Nanosatellites) program, which selects university satellites for launch based on mission relevance, has likely influenced the notable increase in S-, T-, and C- class satellites to the majority of university missions (Swartwout, 2013).

The majority of CubeSat failures through 2012 have been university-led projects (Swartwout, 2013). It is believed that most failures are due to configuration or interface failures that could have easily been avoided if the satellite had been operated under flight-

like conditions prior to launch (Swartwout, 2013). If additive manufacturing can decrease integration time and cost during the satellite build, then the additional resources could be used for system-level functional tests that could catch the majority of errors leading to CubeSat failures prior to launch.

Development and Life Cycle

The general process for spacecraft development can be applied to CubeSats. The spacecraft development process spans from program start to space vehicle launch, and consists of three major processes: the space mission engineering process, the spacecraft design process, and the payload design process (Wertz et al., 2011).

The space mission engineering process is an iterative process that spans program start to requirements definition (Wertz et al., 2011). The main output of this process is the definition of system requirements and allocation of these requirements to system elements, as these requirements will be used to begin the spacecraft design and payload design processes (Wertz et al., 2011). The space mission engineering process can be either need-driven or capability-driven (Wertz et al., 2011). The need-driven process has a specific set of mission objectives and the goal of the spacecraft is to achieve these objectives (Wertz et al., 2011). Instead of mission objectives, the capability-driven process has a goal of developing and demonstrating game-changing, breakthrough technology (Wertz et al., 2011). While many of the applications of additive manufacturing to spacecraft design discussed later in this paper would likely remain capability-driven for the foreseeable future, because the methodology of this work assumes that the technologies to 3D print satellites are already in place, this work will

take a need-driven perspective to analyze the utility of 3D printed CubeSats for satellites with real mission objectives.

According to Wertz and colleagues, the four broadly defined steps of the need-based space mission engineering process are:

1. Define objectives and constraints
2. Define alternative mission concepts or designs
3. Evaluate the alternative mission concepts
4. Define and allocate system requirements (Wertz et al., 2011)

The definition and allocation of system requirements resulting from the space mission engineering process form the starting point for both the spacecraft design and payload design processes. Wertz and colleagues document the steps of the spacecraft design process as:

1. Document design drivers and requirements, including payload parameters
2. Determine overall configuration and key trades
3. Partition into subsystems
4. Establish budgets and subsystem requirements
5. Develop subsystem designs
6. Evaluate overall system configuration against requirements and constraints
7. Explore options
8. Document and iterate steps 1 through 7 (Wertz et al., 2011)

The major design drivers for the spacecraft design process are mass, power, cost, schedule, lifetime and reliability, total delta V (or the measure of impulse necessary to

perform a maneuver in m/s), orbit, and payload accommodation (Wertz et al., 2011). The review of recent work in the development of additive manufacturing for spacecraft that follows this CubeSat overview will focus on tying the research in this area to these major design drivers. The requirements from the space mission engineering process and the spacecraft design process itself take into account the requirements of the CubeSat lifecycle, from the rigors of launch through operation in the harsh space environment and even end-of-life considerations.

Subsystems

The major subsystems of a CubeSat are analogous to those of any other satellite and include propulsion, attitude determination and control system (ADACS), trajectory navigation and control (TNC), on-board processing, the telemetry, tracking, and command (TT&C) system, power, structures, and thermal control system (Wertz et al., 2011). The purpose of the propulsion subsystem is provide thrust to change the spacecraft's orbit and dump momentum as needed (Wertz et al., 2011). The ADACS and TNC subsystems comprise the spacecraft's control systems (Wertz et al., 2011). ADACS determines and controls the orientation of the CubeSat in three-dimensional space, while TNC determines and controls the translational path of the spacecraft in terms of position and velocity (Wertz et al., 2011). The on-board processing subsystem is comprised of the spacecraft computer and associated software that control the operations of the spacecraft, including the control systems and any operations necessary to achieve the mission objectives (Wertz et al., 2011). The TT&C subsystem allows the spacecraft to communicate with the ground station and radiometrically track the spacecraft position relative to the ground station to aid in orbit determination (Wertz et al., 2011). The

power subsystem provides and controls the distribution of electrical power to all spacecraft subsystems (Wertz et al., 2011). The structures and mechanism subsystem and the thermal control subsystem comprise the structures and thermal group of subsystems (Wertz et al., 2011). The structures and mechanism subsystem is the mechanical system of the spacecraft that includes housing and placement of all subsystems and any mechanisms, such as actuators to deploy solar panels (Wertz et al., 2011). The thermal control subsystem controls the temperature of the spacecraft and its components to keep them all within the range of operating temperatures (Wertz et al., 2011).

Space Applications of Additive Manufacturing

In addition to matching the research in the area of space applications of additive manufacturing to the spacecraft design drivers, this section will also relate AM research to the CubeSat subsystems. Doing so will help begin to identify the areas of CubeSat development and specific subsystems that have the highest likelihood for being impacted by the additive manufacturing of CubeSats.

Before specific applications of additive manufacturing in the space environment can be considered in detail, it should first be shown that the materials used in the process are suitable for the space environment as part of the lifetime and reliability design driver and the structures and mechanisms subsystem. Gutierrez and colleagues performed an outgas testing experiment to demonstrate the capability of AM materials to participate in spaceflight (Gutierrez et al., 2011). The team focused on fused deposition modeling (FDM), examples of which are thermoplastics and extrusion methods; stereolithography (SLA) materials were used for comparison (Gutierrez et al., 2011). All of the FDM

materials chosen for testing were thermoplastics selected for their strength and durability (Gutierrez et al., 2011). The materials tested were 0.18mm layer thickness of acrylonitrile butadiene styrene (ABS), a material with strong layer bonding; ABS-M20, a type of ABS thermoplastic; 0.18mm layer thickness of polycarbonate (PC), a material with good mechanical properties and heat resistance; PC-ABS, a PC and ABS thermoplastic; and 0.25mm layer thickness of ULTEM, a flame, smoke and toxicity (FST) certified material with high heat resistance (Gutierrez et al., 2011). All materials were exposed to a 6×10^{-7} Torr pressure representing the vacuum environment of space, and all materials showed less than 1% outgassing, thus passing NASA requirements of 1% or less (Gutierrez et al., 2011).

A review of the literature demonstrates a focus on three main areas of AM techniques applied to satellite development: embedded electronics, thrusters, and radiation hardened materials. These three areas of interest are discussed in detail, including relationships to the spacecraft design drivers and the CubeSat subsystems, in the following sections.

Embedded Electronics

In this work embedded electronics are defined as electronic circuits and components that have been built directly into an AM satellite structure, thus taking advantage of AM's unique layer-by-layer process to build the electronics directly into the CubeSat's structures subsystem and eliminate the volume required by electronics cards. Embedded electronics have the potential to impact the power, cost, schedule, lifetime and reliability, and payload accommodation spacecraft design drivers in CubeSat development. In particular, they could decrease cost and schedule by reducing the

amount of time spent dealing with messy wiring harnesses, and could make payload accommodation easier by utilizing unique geometries to optimize the volume required for the power subsystem, thus increasing the volume available for the payload. Embedded electronics would impact the power, structures, and thermal control subsystems of a CubeSat, the latter due to the need to remove heat from the enclosed electronic components that may otherwise be trapped in the structure.

Like typical satellites a CubeSat relies on printed circuit boards (PCBs) for electronic components. The physical form PCBs is confined to flat, two-dimensional surfaces, making it difficult to optimize a satellite's size and weight without changing the boards. Gutierrez et al proposed 3D-printing circuits, using the techniques of additive manufacturing, robotic pick-and-place, and direct print (DP), directly into structures, thus allowing for optimization of existing volumes (Gutierrez et al., 2011). A review of previous work in this area began with the addition of channels to the substrate for placement of the conductive material (Gutierrez et al., 2011). The use of channels to place the conductor virtually eliminates electrical shorts and also means that the line spacing of the conductive material is controlled by the SLA process instead of DP (Gutierrez et al., 2011). Initially, however, this method used planar faces, not conformal surfaces, and was demonstrated with a functional programmable intelligent computer (PIC) processor, global positioning system (GPS), and radio frequency (RF) (Gutierrez et al., 2011). Another team looked further into building channels for conductive material; their effort was successful in the horizontal direction, but unsuccessful in the vertical direction (Gutierrez et al., 2011). Yet another team developed a cylindrical magnetometer with surface-mounted electronics, notable for the placement of electronics

on a conformal (cylindrical) surface (Gutierrez et al., 2011). This work was expanded upon by the development of the ability to print conductive lines of metal-based inks with a width of down to 25 microns at a speed of up to 250 mm/s onto 3D conformal surfaces, not just planar processing (Gutierrez et al., 2011).

Traditional electronics computer aided design (CAD) programs are optimized for 2D PCB technology, and so are not very useful for 3D structural electronics (Gutierrez et al., 2011). As a result, the methodology proposed in Gutierrez involved sketching electronics implementation details by hand and rendering the device in mechanical CAD (SolidWorks) to show the cavities and channels that will isolate the conductive material (Gutierrez et al., 2011). The CAD model was transferred directly to the 3D printer as an STL (STereoLithography) file (Gutierrez et al., 2011). A post-processing program was used to determine build orientation, layering, and so on, to include component insertion and micro-dispensing information (Gutierrez et al., 2011).

Gutierrez and colleagues then went on to lay the conductive ink Ercon 1660 on SLA material (Gutierrez et al., 2011). After demonstrating functionality, the circuits were exposed to a 6 x 10^-7 Torr "vacuum" pressure, again representing the vacuum environment of space (Gutierrez et al., 2011). All circuits proved to still be functional after the outgassing test (Gutierrez et al., 2011).

Medina and colleagues sought to create a fully functional electromechanical device with AM techniques, without having to remove the piece from the build plate and re-register it (Medina et al., 2005). The work combined SLA and direct write (DW) technologies (Medina et al., 2005). DW was used to add conductive ink was added to SLA material while still on the SLA build plate (Medina et al., 2005). The laser from the

SLA system was used to cure the DW conductive ink on the SLA plate, then the build continued without having to move the part from the build plate (Medina et al., 2005).

While AM methods have been shown to produce more compact, reliable, and less expensive circuitry, there were a number of process issues, including the adhesion of the conductor and the SLA resin and the curing of the conductive ink (Medina et al., 2005). Many available SLA resins cannot take the temperatures, often over 100°C, required to cure DW conductive inks (Medina et al., 2005). The method proposed by Medina was enabled by relatively recent developments in high-temperature resins such as ProtoTool, ProtoTherm, and NanoForm by DSM Somos (Medina et al., 2005). In addition, previous efforts to combine DW and SLA to print circuitry required that the part be removed from the SLA machine, cleaned, and cured prior to the DW process (Medina et al., 2005). After DW, the part must be returned to the SLA platform and re-registered prior to continuing the build (Medina et al., 2005). Avoiding the necessity of removing the part from the SLA platform provided the motivation for Medina's design of an automated hybrid system (Medina et al., 2005).

Medina's Functional Integrated Layered Manufacturing (FILM) concept for a semi-automated hybrid SLA/DW machine combined AM techniques with other manufacturing technologies in an automated process to take advantage of multiple capabilities to produce a functional device (Medina et al., 2005). In this process, the SLA build is stopped for the application of conductive ink with DW, but the component is not removed from the build platform (Medina et al., 2005). The DW material is then cured with the SLA laser, and the build is continued without having to re-register the part since the component never left the SLA platform (Medina et al., 2005). The set-up for

demonstration started with a 3D Systems 250/50 SLA machine, with a laser upgraded to 355nm solid-state (Medina et al., 2005). The SLA material used for the demonstration was DSM Somos ProtoTherm 12120 (Medina et al., 2005). The material was selected for its high heat deflection temperature of 126°C which allowed it to withstand the DW ink cure, and for its relatively low viscosity (550 centipoise) to improve the handling, building without sweeping, and cleaning prior to the DW part of the process (Medina et al., 2005). A custom adjustable height table was built to align the DW system with the SLA rim support plate (Medina et al., 2005). Automatic linear stages controlled with LabView on this adjustable bench provided X-Y axes movement, and a manual linear stage on the adjustable benched provided Z axis movement (Medina et al., 2005). The EFD Inc. 2405 Ultra Dispensing System was selected as the DW system for this demonstration (Medina et al., 2005). The DW system was adapted for conductive ink CI-1002 by ECM; this ink was selected for its low cost and low cure temperature of only 110°C for 2 hours in 15-minute intervals (Medina et al., 2005). Ink dispensing was also controlled with LabView, and the dispensing tip size and dispensing pressure were optimized to obtain the narrowest continuous line possible, determined to be 0.014" (Medina et al., 2005). To register the DW trace with the SLA laser for curing, a small reference hole was made during the SLA build for registering the DW ink tip; this hole was later filled with conductive ink to provide a vertical interconnection between electrical layers to produce 3D electronics (Medina et al., 2005).

To demonstrate the hybrid SLA/DW automated machine, the STL file was divided into 5 distinct parts—3 for the SLA part of the build, and 2 for the DW part of the build (Medina et al., 2005). SLA part 1, with the reference hole, was built on the SLA

platform (Medina et al., 2005). The SLA resin vat was then lowered and protect from the DW cure with a UV shield (Medina et al., 2005). The top surface of the built component was cleaned with alcohol, although it could be further laser cured to ensure no contamination between resin and ink (Medina et al., 2005). The DW nozzle was then aligned with the reference hole and the DW circuit part 1 was laid down (Medina et al., 2005). To cure the ink, the laser power was increased with an attenuator in the beam path and the penetration depth was decreased to reduce the laser traverse speed and increase localized heating (Medina et al., 2005). Once the DW process was complete for DW part 1, the SLA component was cooled to a specified temperature, the vat was raised, the laser power was reduced, so that SLA part 2 could be built as previously on top of the DW circuit layer (Medina et al., 2005). This same process was repeated to produce DW circuit part 2 and SLA part 3 (Medina et al., 2005). The reference hole filled in with conductive ink electrically connected DW circuit parts 1 and 2, thus producing a 3-dimensional circuit (Medina et al., 2005).

Lopes and colleagues demonstrated the functionality of embedded circuits built with the semiautomatic hybrid SLA and DW machine described previously by building a temperature-sensitive circuit with many commonly used components and comparing its functionality to that of the same circuit built with PCB technology (Lopes et al., 2006). Their motivation was to reduce size by placing components within complex geometries and by layering 3D circuits instead of placing components side-by-side. In addition, embedding components can increase the strength of the circuit and protect it from outside hazards, compared to traditional PCB technology (Lopes et al., 2006). High volume PCB manufacturing "can be expensive and wasteful" relative to AM technology, which

requires fewer steps thus reducing manufacturing costs (Lopes et al., 2006). In addition, AM increases design flexibility and has minimal waste because it is an additive instead of subtractive process (Lopes et al., 2006).

Upgrades to the automated hybrid system for this demonstration included precision linear positioning stages with built-in 0.1 micron resolution linear encoders for 3-axis XYZ movement (Lopes et al., 2006). The conductive ink E1660-136 by Ercon was selected for this demonstration for its low curing temperature (138°C for 15 minutes) and its low resistivity, which at 0.011 Ω/square/mil was the lowest of all samples measured (Lopes et al., 2006). In addition, measurements between different inks on different substrates showed that this ink had the lowest average resistivity after the thermal cure on all tested substrates (Lopes et al., 2006).

The circuit chosen for demonstration was a 555 timer circuit. Components included a battery holder, LM555 timer chip, 3 resistors, a thermistor, a capacitor, a switch, and 2 LEDs which oscillate in time with the timer chip, so they operate at a frequency proportional to the thermistor temperature (Lopes et al., 2006). To build this circuit, an SLA component with sockets for embedding electronic components was built, with a pause in the build to manually insert components (Lopes et al., 2006). The components were then embedded in the SLA piece by continuing the building (Lopes et al., 2006). The top surface had vertical connector holes for the conductive material to access the component pins (Lopes et al., 2006). The conductive ink was then laid down with DW, and a heat convection oven was used to cure the ink (Lopes et al., 2006). The AM demonstration circuit and a PCB circuit with the same components were tested at the same time (Lopes et al., 2006). The two circuits were exposed to temperatures that

ranged from -20°C to 90°C in 10°C increments and held at that temperature for 5 minutes prior to measurements to achieve thermal stability (Lopes et al., 2006). The resistances and capacitances that affect frequency were measured at each temperature increment (Lopes et al., 2006). The comparison resulted in ±1% variation between resistances and capacitances of the two different circuits, which was well within the ±10% tolerances of the components themselves, leading to the conclusion that the differences between the two circuits were most likely due to component variation, not differences in the manufacturing processes (Lopes et al., 2006).

Lopes and colleagues did note that at less than 10mW the 555 timer circuit is a low power consumption system so there is no appreciable heat generation (Lopes et al., 2006). Heat generation could become an issue for circuits with high power consumption from self-heating of the circuit due to embedded components (Lopes et al., 2006). The team suggested leveraging AM's ability to produce unique geometries by researching passive cooling techniques such as built-in heat pipes and other forms of advanced thermal management (Lopes et al., 2006).

Navarrete and colleagues used the semi-automatic hybrid SLA/DW machine as described previously to build a functional object for a specific application, rather than another proof-of-concept (Navarrete et al., 2007). The goal was to produce a durable, difficult-to-detect, and reverse-engineering resistant motion sensor for border patrol applications (Navarrete et al., 2007). Using AM techniques and embedded 3D electronics to build the sensor resulted in a product that easily met all of the application requirements (Navarrete et al., 2007). In addition to the motion sensor, the embedded package include navigation capabilities with a GPS receiver and the ability to

communicate over unregulated radio frequency transmission (Navarrete et al., 2007). Because of 3D-printing's capability to produce unique geometries, the resulting sensor package was rock-shaped for blending into the background (Navarrete et al., 2007).

Constraints on the motion sensor design included minimizing the number of components to reduce embedding requirements (Navarrete et al., 2007). The minimum electronic component pin pitch requirement was limited by the DW ink trace width (Navarrete et al., 2007). Low power and low frequency components were also preferred to minimize heat dissipation requirements due to embedding the components in SLA material (Navarrete et al., 2007).

Perez reviewed the methods, advantages, and issues with integrating electronics into the structure of an object with additive manufacturing techniques (Perez et al, 2013). The three DW processes discussed are extrusion methods, ink jetting, and aerosol jetting (Perez et al, 2013). Extrusion methods require precise control over the positive dispensing pressure which directly affects the feature widths (Perez et al, 2013). This method is able to achieve feature widths down to 25 microns and speeds of up to 300 mm/s, although 50 mm/s is more typical (Perez et al, 2013). Extrusion methods typically dispense metal-based inks, with a conductivity of about 10^5 S/m as deposited, increasing to about 10^7 S/m with sintering (Perez et al, 2013). Ink jetting methods are based on expelling droplets and can achieve features down to 20 microns (Perez et al, 2013). A single nozzle dispenses only 0.3 mm^3/s, although the rate can be increased by using an array of nozzles (Perez et al, 2013). An advantage of this method is drop by drop control for discrete placement of the conductive path (Perez et al, 2013). As in extrusion methods, the conductivity can be improved by sintering (Perez et al, 2013). Aerosol

jetting methods use a vapor stream to deposit material (Perez et al, 2013). This method results in the smallest feature size, down to 10 microns and a single pass thickness of up to microns (Perez et al, 2013). However, the deposition rate is only 0.03 mm^3/s at an extrusion-level resolution of 50 microns (Perez et al, 2013).

Some of the issues with integrating DW and AM are the sintering temperatures required to maximize ink conductivity are incompatible with the heat deflection temperature of many AM materials (Perez et al, 2013). Only a few AM polymers, such as Duraform HST for selective laser sintering (SLS) machines, Prototherm for SLA machines, and ULTEM for FFF machines can withstand the 100°C minimum temperature required to sinter many metal inks (Perez et al, 2013). The temperatures required for sintering can be decreased by decreasing the metal particle size of the conductive material to the nanoscale (Perez et al, 2013). However, particles of this size tend to agglomerate, causing clogs (Perez et al, 2013). Coating the particles with capping agents can prevent agglomeration and subsequent clogs, but unfortunately the capping agents also require high temperatures for removal (Perez et al, 2013). Another method is to use pulsed photonic curing, which heats traces without damaging the polymer substrate (Perez et al, 2013). This method only works for planar, not conformal, surfaces, due to the criticality of distance to the process, and it only allows thin layer heights (Perez et al, 2013).

Adhesion between the conductive material and the substrate, between the conductive layers, and to external circuitry is also a concern (Perez et al, 2013). Several key factors contribute to the adhesion of DW materials to AM substrates, such as the surface energy of both materials, the substrate surface roughness, the substrate surface

treatment, and the chemical interactions between both materials (Perez et al, 2013). For example, fused filament fabrication (FFF) results in a highly non-uniform, ridged surface (Perez et al, 2013). When DW techniques are applied, the conductive inks tend to fill the valleys between the ridges (Perez et al, 2013). Wicking of the conductive inks through the valleys is also an issue, as it can lead to short circuits and other discontinuities (Perez et al, 2013). These issues can be addressed with a dielectric bonding layer between the substrate and ink (Perez et al, 2013). The dielectric bonding layer is also helpful even on smoother surfaces such as those produced through SLA (Perez et al, 2013). In addition, the dielectric bonding layer reduces stresses from any mismatch in coefficient of thermal expansion (CTE) between the plastic substrate and the metal ink (Perez et al, 2013).

Thrusters

An examination of AM embedded or 3D printed thrusters indicates that they have the potential to impact the mass, power, total delta V, and orbit design drivers. AM thrusters are of interest not only in the propulsion subsystem but also in attitude determination and control.

Marshall and colleagues set forth to embed a commercial micro pulsed plasma thruster into 3D printed material and demonstrate thruster functionality after the printing process (Marshall et al., 2015). Marshall points to the increased use of CubeSats for missions previously performed only by larger satellites because they are “ready-to-build” systems that provide relatively easy access to space (Marshall et al., 2015). Part of the team’s goal of incorporating additive manufacturing into CubeSat builds is to increase customizability of these systems (Marshall et al., 2015).

The team's focus was on a thruster system intended for attitude control (Marshall et al., 2015). CubeSats commonly use magnetic torque rods and momentum wheels for attitude control, although both of these systems have limitations (Marshall et al., 2015). Magnetic torque rods limit CubeSats to LEO because they depend on the Earth's magnetic field, preventing CubeSats from being considered for missions at higher orbits or possibly even lunar or planetary missions (Marshall et al., 2015). Momentum wheels tend to saturate and require a secondary system to desaturate them to a usable level, which takes up valuable space on a small satellite (Marshall et al., 2015). As a result, both systems are limiting if CubeSats are to continue in the trend of taking on missions intended for larger satellites, particularly for missions outside of LEO (Marshall et al., 2015).

The team considered printing a cold-gas propulsion system, which uses a pressurized tank to expel gas through a nozzle for thrust (Marshall et al., 2015). However, most propellants require a high pressure such that the material layers in the AM process must be very tightly sealed (Marshall et al., 2015). This tight seal is achievable through SLA methods but not through the material extrusion process intended for use in this demonstration for its relative ease of embedding electronics (Marshall et al., 2015). The result was the selection of a Busek micro-pulsed plasma thruster for the demonstration (Marshall et al., 2015). These thrusters work by applying a voltage across the thruster's electrodes to form a spark (Marshall et al., 2015). The spark then vaporizes a small amount of the electrode, and the expelled material provides the desired thrust (Marshall et al., 2015).

The demonstration was largely concerned with answering two main questions. The first was whether a 3D printed material could provide sufficient dielectric strength to prevent arcing through the material when the voltage is applied to the thruster (Marshall et al., 2015). The second was whether or not the thruster could withstand the high temperatures in the printing process and be able to operate as anticipated after embedding in the material (Marshall et al., 2015). To answer the first question, the team investigated the dielectric strength of polycarbonate printed materials by applying a voltage and measuring the resistance; a decrease in resistance is an indicator that arcing has occurred through the printed material (Marshall et al., 2015). Measurements showed that arcing occurred in the 7.5-10 kV range, providing significant margin for the expected thruster operating voltage of 1.5 kV (Marshall et al., 2015). To address the second question, the team 3D printed a thrust panel with a single thruster and conductive traces embedded into the panel (Marshall et al., 2015). This thrust panel was tested and operated under vacuum (about 10^{-5} torr), demonstrating proof-of-concept operation (Marshall et al., 2015). The thruster firing did not degrade the material around the thruster (Marshall et al., 2015). However, the team observed material discoloration that suggested arcing between one of the wires and the thruster, although this did not impact the operation of the thruster and is anticipated an addressable issue in future work (Marshall et al., 2015).

The RAMPART (RApidprototyped MEMS Propulsion and Radiation Test) 2U CubeSat was intended to demonstrate warm gas propulsion subsystems for CubeSat altitude adjustment alongside the printing of satellite structures, including the propulsion system, at less cost than current CubeSat manufacturing methods (Moore et al., 2010). Because CubeSats are often a secondary payload, they are not always placed in the

optimal orbit for their mission (Moore et al., 2010). The purpose of the RAMPART propulsion system design is to provide enough thrust in a 1U volume that can attach to a 1U or 2U CubeSat to adjust the satellite's altitude to a more favorable position (Moore et al., 2010). The team designed a warm gas propulsion system for fabrication with Windform, a laser sintering material used in Formula 1 racing (Moore et al., 2010). The design uses a non-flammable, non-toxic compressed liquid propellant that has its specific impulse raised by heating just prior to exiting the nozzle (Moore et al., 2010).

Radiation Hardened Materials

The development of radiation hardened materials for use in 3D printing satellites has the potential to impact the mass, lifetime and reliability, and orbit design drivers, particularly for the structures and thermal control subsystems. There exist two main methods for radiation shielding of small satellites such as CubeSats. The first is to use electronic parts that have either already been radiation hardened or that have intrinsic shielding; these components are often considerably more expensive than "regular" components (Kwas et al., 2014). The second method is to use shielding material to prevent radiation from reaching the electronic components by attenuating the radiation (Kwas et al., 2014). However, the effectiveness of the shielding material is often proportional to its thickness, which results in increased mass and decreased volume available for mission-specific components (Kwas et al., 2014). In addition, the atomic mass of materials correlates to their effectiveness of shielding against radiation (Kwas et al., 2014). Thermoplastics, which are low atomic mass materials, shield against protons and neutrons, while tungsten and tantalum, which are high atomic mass materials, shield against electrons (Kwas et al., 2014). Additive manufacturing has the potential to

combine these materials to obtain the shielding properties of both low- and high-atomic mass materials by either alternating layers of the different materials or combining the materials into a new filament stock (Kwas et al., 2014).

Kwas and colleagues addressed two main investigative questions for using additive manufacturing to combine materials of different shielding properties to improve overall shielding performance (Kwas et al., 2014). The first was whether or not these hybrid materials could be printed with the two suggested AM methods (Kwas et al., 2014). The second was whether the resulting product would behave as predicted in terms of shielding effectiveness (Kwas et al., 2014). The team printed CubeSat size panels with a variety of materials and tested them with low-energy X-rays (Kwas et al., 2014). The materials used for printing the panels were polycarbonate (PC), ULTEM, PC-ABS, PC-ESD (electrostatic discharge), nylon, ABS with 2% tungsten, ABS with ultra-high-molecular-weight polyethylene, and PC with 1%, 3%, and 5% tungsten (Kwas et al., 2014). The results of the low-energy X-ray tests showed the highest shielding effectiveness from PC and ABS samples with a percentage of tungsten (Kwas et al., 2014). In fact, the plain PC sample improved from about 90% to about 98% attenuation factor when 5% tungsten was added (Kwas et al., 2014).

Summary

The available literature supports the assertion that space applications of additive manufacturing have the potential to impact all of the major spacecraft design drivers for CubeSats and many of the main subsystems. In addition, the research discussed in the preceding sections provides justification for the methodology assumption that it is

possible to fully print a CubeSat bus, including embedded electronics, thrusters, and radiation shielding—although the technology is not there yet for a fully printed CubeSat bus, there is ample evidence to suggest that such an architecture is within the realm of feasibility. The three main areas of interest as identified in the available research are AM embedded electronics, printed or embedded thrusters, and radiation hardened materials.

III. Methodology

Chapter Overview

The purpose of this chapter is to describe how this work will quantify the impact of using AM techniques in the areas of embedded electronics, thrusters, and radiation hardened materials. The proposed benefits in each area of interest are identified in this chapter, followed by an AV-1 summarizing the simple printed CubeSat architecture and its purpose. Finally, this chapter will describe how the architecture summarized in the AV-1 will be quantitatively analyzed and will show the development of quantitative data-based predictive models.

Overview of Research Methodology

The methodology begins with the development of a printed CubeSat architecture that maps the proposed benefits of AM in each area of interest to CubeSat subsystems, advantages offered by utilizing AM techniques, and the measures for a quantitative assessment. Based on this mapping in the architecture, quantitative risk models will be developed in Analytic Solver Platform for Excel to determine the impact of each potential benefit on the development of the CubeSat system using the measures identified in the architecture. The analysis and results of these models will provide a starting point

for decision makers to discuss whether a printed satellite architecture merits investment, outside the scope of this work.

Description of Proposed Benefits

The three main areas of interest as identified in the literature review are embedded electronics, printed or embedded thrusters, and radiation hardened materials. This work will examine one or more of the proposed benefits for a CubeSat system in each of these areas of interest. The area of embedded electronics has three proposed benefits that will be considered in this work. The first two proposed benefits are that embedded electronics can enable a smaller CubeSat to perform the mission and can increase the volume available for the payload by decreasing the volume required for the CubeSat's electronics. The third is that embedded electronics can decrease the time spent in integration by eliminating the need for messy wiring harnesses. The area of printed or embedded thrusters has two main proposed benefits. First, embedding small thrusters into the satellite structure to decrease the volume and mass required for ADACS can enable a smaller CubeSat to perform the mission, and second, using AM techniques to build new CubeSat-scale propulsion designs can enable the CubeSat to achieve a more desirable orbit after being launched into a less desirable orbit as a secondary payload. New propulsion designs enabled by AM have the potential to result in a smaller propulsion system with a higher delta V, which increases the orbit change options available to the CubeSat. The proposed benefit for AM radiation hardened materials is that building radiation shielding directly into the structure to reduce the mass of the CubeSat can enable a lighter CubeSat to perform the mission.

Model Design

Printed Satellite Architecture Development

The purpose of the Benefit Evaluation of Additive Manufactured (BEAM) CubeSat architecture is to show the relationships between the three areas of interest, their proposed benefits, the CubeSat subsystems impacted by the proposed benefits, how AM enables each proposed benefit, and the measures that can be used to quantify the impact of each potential benefit on the CubeSat system. The AV-1 shown in Table 1 summarizes the BEAM CubeSat architecture that is to be analyzed.

Table 1. Overview and Summary Information (AV-1) for BEAM CubeSat

Architecture Project Identification	
Name	*Benefit Evaluation of Additive Manufactured CubeSat (BEAM CubeSat)*
Description	*BEAM CubeSat is a hypothetical small satellite with key components manufactured and integrated with additive manufacturing (3D printing). The purpose of the BEAM CubeSat is to evaluate the proposed benefits of additive manufacturing in the areas of embedded electronics, thrusters, and radiation hardened materials.*
Architect(s)	*Rachel Sharples*
Organization	*Air Force Institute of Technology (AFIT)—SENG 799 Independent Study*
Assumptions and Constraints	- *The technology to manufacture and integrate key components of a CubeSat with 3D printing is achievable.* - *Embedding electronic components and 3D printing electrical connections does not decrease the power available to the CubeSat.* - *Thermal management of any increase in heat due to embedding of electronic components is resolved.* - *Temperatures required for curing conductive material are compatible with the AM substrate.*

	- *Conductive material fully adheres to AM substrate.* - *CubeSats will continue to be launched as secondary payloads and will be placed in the same orbit as the primary payload.* - *Small thruster technologies will continue to be available.* - *Thrusters can be electrically connected via embedded electronics.* - *Radiation hardened materials for AM can achieve radiation shielding equivalent to that of conventional methods.*
Approval Authority	*Lieutenant Colonel Jeffrey Parr* *Dr. David Jacques* *Dr. Leslie Vaughn*
Date Completed	*Final architecture to be released NLT Sept 15*
Estimated Costs	*300 hours*
Scope: Architecture Views and Models Identification	
Views Developed	*- AV-1 (Overview and Summary Information)* *- OV-5a (Operational Activity Decomposition Tree)* *- SV-1 (Systems Interface Description)* *- SV-4 (Systems Functionality Description)* *- SvcV-1 (Services Context Description)* *- SvcV-3a (Systems-Services Matrix)* *- SvcV-5 (Operational Activity to Services Traceability Matrix)* *- SvcV-7 (Services Measures Matrix) *
Time Frames Addressed	*Estimated 10-20 years to maturation of AM technology*

Organizations Involved	- US Air Force - Air Force Space Command (AFSPC) - Joint Space Operations Center (JSpOC) - Launch Support - Contractor Developers - University Researchers
Purpose and Viewpoint	
Purpose (Problems, Needs, Gaps)	*Using AM technology to print a satellite has many areas of proposed benefit, to include reducing size, weight, and power (SWaP) by embedding electronics and sensors directly into the spacecraft structuring, enabling previously impossible propulsion designs by utilizing AM's ability to create unique geometries that are not achievable with traditional manufacturing techniques, and building radiation protection directly into the spacecraft structures by developing radiation-hardened printable materials. From a system perspective, if all of these proposed benefits were true, the key components of the BEAM CubeSat would be manufactured using 3D printing. The BEAM CubeSat would have all of the electronics and sensors embedded in radiation hardened material and an integrated propulsion system that is part of the satellite itself. The printed components of the BEAM CubeSat would have a smaller volume. Because most of the satellite is already printed as a single item, minimal integration is required, thus decreasing development time. BEAM CubeSat is a case study to provide a quantitative analysis of the actual impact of some of these proposed benefits throughout the CubeSat development and life cycles, which outside the scope of this work will feed into the discussion of whether or not additive manufacturing technology for satellites is worth Air Force investment.*
Questions to be Answered	1. *What would a 3D printed CubeSat architecture look like?* 2. *On what CubeSat subsystem, if any, would a 3D printed CubeSat architecture have the greatest impact?* 3. *Which of the proposed benefits of 3D printing, such as optimization of mass and volume using embedded electronics, the ability to produce unusual geometries for unique propulsion and attitude control systems,*

	and increased radiation protection from embedding components in custom materials, would have the greatest impact on a 3D printed CubeSat launch?
Architecture Viewpoint	*The BEAM CubeSat architecture will be developed from the perspective of the developer of a CubeSat.*
Context	
Mission	*The mission of the BEAM CubeSat is to provide a case study for evaluation of AM techniques in satellite development and manufacturing.*
Doctrine, Goals and Vision	*Utilize AM techniques to enable a more cost-effective solution to satellite manufacturing.*
Rules, Conventions and Criteria	*The BEAM CubeSat architectural data conforms to the DoD Architecture Framework (DoDAF) Version 2.0.*
Linkages to Other Architectures	*Once proven the BEAM CubeSat architecture can be linked to the architecture of other CubeSats whose developers are interested in evaluating the impact of AM technology on satellite development.*
Tools and File Formats to be Used	
Sparx Enterprise Architect v10.0, Microsoft Word 2013, Microsoft Excel 2013, Analytic Solver Platform for Excel 2013, Microsoft PowerPoint 2013.	

Quantitative Risk Models

The views for the BEAM CubeSat architecture described in the preceding AV-1 emphasize mapping between services, operational activities, systems, and measures. The proposed benefits will be defined as the services in the services context description (SvcV-1), the advantages offered through AM techniques will be defined as the operational activities in the operational activity model (OV-5a), and the CubeSat subsystems will be defined as the systems in the SV-1. For the quantitative analysis,

each service will be analyzed according to the corresponding measures in the services-measures matrix (SvcV-7). Data from CubeSat kit and component manufacturers will be used to develop a predictive model for each measure, thus quantifying the impact of each proposed benefit on the CubeSat system.

Assumptions

The BEAM CubeSat AV-1 shown in Table 1 lists the assumptions for this work.

Statistical Methods and Analysis

CubeSat Volume and Mass Modeling

To determine the percent reduction in the volume and mass of the overall spacecraft, the volume and mass of CubeSats of varying sizes must first be known. This analysis considered 1U, 2U, 3U, and 6U CubeSats, where 1U is a cube 10cm on an edge, with a constant volume of 1,000,000 mm^3. For CubeSats 3U or less, the mass was modeled as a constant 1.33 kg per 1U (Thompson, 2015). 6U satellites have a larger variation in weight, generally ranging from 12 to 14 kg (Thompson, 2015). As a result, the mass of the 6U satellite was modeled as a truncated normal distribution with a mean of 13 kg, a minimum cutoff of 12 kg, a maximum cutoff of 14 kg, and a standard deviation of 0.5 kg, as shown in Figure 1.

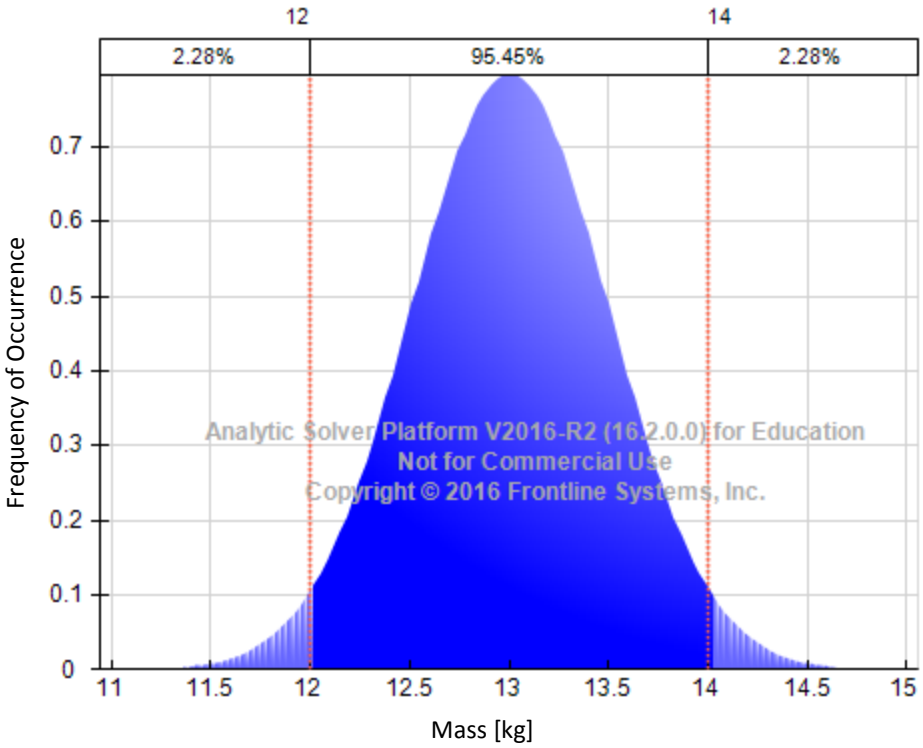

Figure 1. Distribution modeling mass of a 6U CubeSat

Electronics Subsystem Volume and Mass Modeling

The mass and volume data for the electronics subsystem analysis were gathered from the standard CubeSat kits available from Pumpkin, a CubeSat kit manufacturer (CubeSat Kit, 2013). The electronics boards available for these standard CubeSat kits include a pluggable processor module (PPM), a motherboard, a GPS receiver, a battery module, a linear EPS, and an ADACS interface. Pumpkin offers six options for the PPM, three options for the motherboard, two options for the GPS receiver, one option for the battery module, two options for the linear EPS, and one option for the ADACS interface. The spec sheet for each option lists the mass, width, length, board thickness, maximum height of the components above the board, and maximum height of the components below the board. The overall height for determining the volume required for each board

was calculated by summing the thickness of the board, the height above the board, and the height below the board. Table 2 summarizes the data from the spec sheets for each component option, as well as the calculated volume in cubic millimeters and in U.

Table 2. Mass and volume data for Pumpkin CubeSat kit standard electronics boards

Component	Mass [g]	Width [mm]	Length [mm]	Thickness [mm]	Height Above [mm]	Height Below [mm]	Volume [mm3]	Volume [U]
Pluggable Processor Module (PPM)								
A1	11	54.6	53.4	1.6	2	4	22158.86	0.022159
A2	11	54.6	53.4	1.6	2	4	22158.86	0.022159
A3	11	54.6	53.4	1.6	2	4	22158.86	0.022159
B1	16	54.6	89.5	1.6	2	4	37138.92	0.037139
D1	17	54.6	89.5	1.6	2	4	37138.92	0.037139
D2	17	54.6	89.5	1.6	2	4	37138.92	0.037139
Motherboard (MB)								
Option 1	77	96	90	1.6	11.4	3.5	142560	0.14256
Option 2	88	96	90	1.6	12.5	3.5	152064	0.152064
Option 3	103	96	90	1.6	24.5	3.5	255744	0.255744
GPS Receiver (GPSRM1)								
Option 1 (w/o GPS antenna cable connected)	106	96	90	1.6	11	2.75	132624	0.132624
Option 2 (w/ GPS antenna cable connected)	106	96	90	1.6	11	5.5	156384	0.156384
Battery Module	310	96	90	1.6	21.75	1.75	216864	0.216864
Linear EPS								
Option 1 (w/ option /00)	155	96	90	1.6	14	2	152064	0.152064
Option 2 (w/ option /01)	210	96	90	1.6	24	2	238464	0.238464
ADACS Interface	49	90	90	1.6	14	1	134460	0.13446

For the purpose of this analysis, the PPM, motherboard, GPS receiver, battery module, linear EPS, and ADACS interface comprise all of the electronics subsystem considered for embedding. It is assumed that this subsystem stays the same across CubeSats ranging in size from 1U to 6U, so that a 1U CubeSat will have the same mass and volume devoted to the electronics subsystem as a 6U CubeSat. To develop distributions for the mass and volume of the electronics subsystem, first the mass and volume data from the spec sheets were averaged across all options for each of the listed components. The sum of these averages was taken to be the average mass and volume of the electronics subsystem. The sums of the minimum and maximum value options across

all the components were used to define respectively the minimum and maximum mass and volume of the electronics subsystem, which were then used as cutoff values in the distributions modeling the mass and volume of the electronics subsystem. The standard deviation of each distribution was then adjusted so that approximately 95% of the distribution fell between these maximum and minimum cutoff values.

Using this method, the volume of the electronics subsystem was modeled as a truncated normal distribution with a mean of 904,196.9 mm^3, a minimum cutoff of 800,730.90 mm^3, a maximum cutoff of 1,039,055 mm^3, and a standard deviation of 60,000 mm^3. The resulting distribution is shown in Figure 2, with the x-axis units in thousands of mm^3.

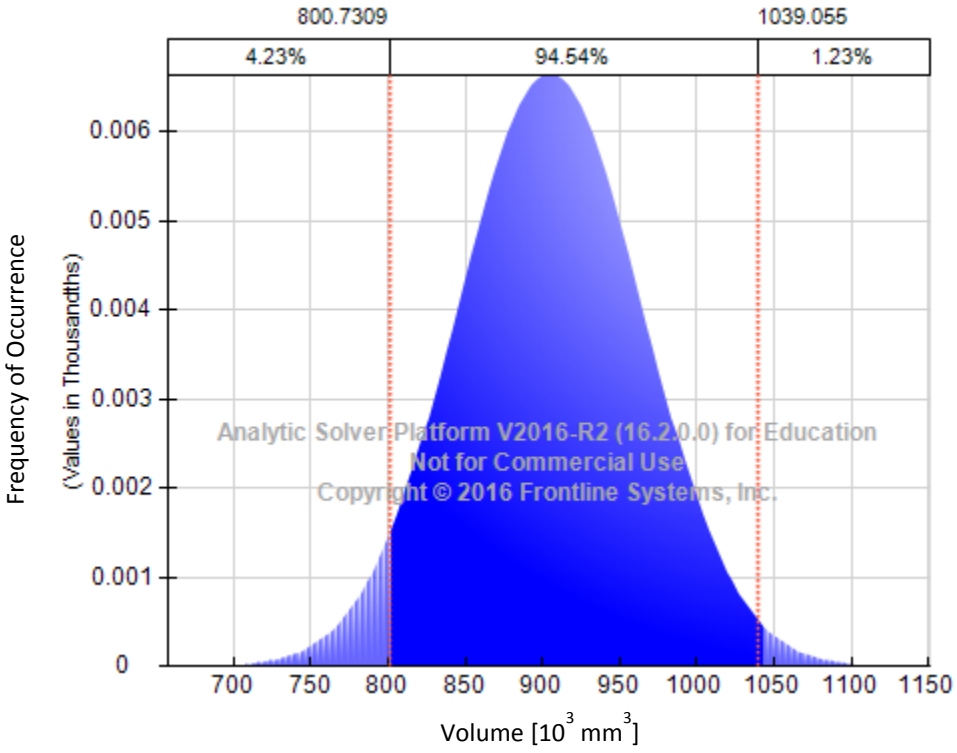

Figure 2. Distribution modeling volume of electronics subsystem

The mass of the electronics subsystem was modeled as a truncated normal distribution with mean 0.751 kg, minimum cutoff of 0.708 kg, maximum cutoff of 0.795 kg, and standard deviation of 0.022 kg, as shown in Figure 3.

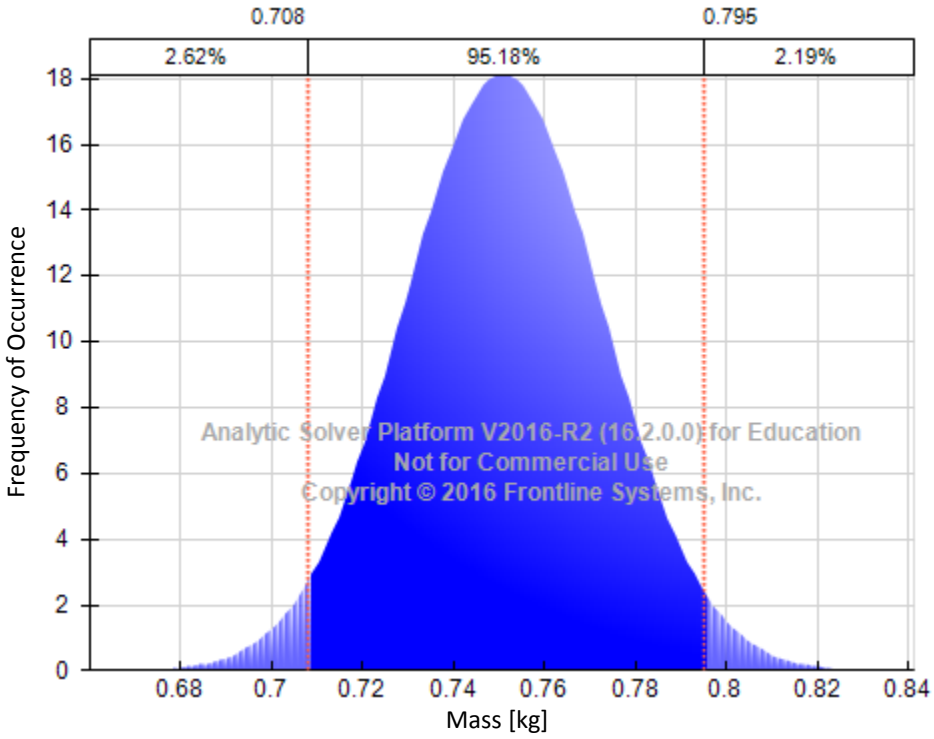

Figure 3. Distribution modeling mass of electronics subsystem

ADACS Volume and Mass Modeling

The mass and volume data for the ADACS subsystem analysis, shown in Table 3, were gathered from standard CubeSat components. The MAI-100 and MAI-200 options are available from Pumpkin, and include separate specifications for ADACS and the magnetometer; the masses and volumes of each of these two subsystems were summed to obtain the overall mass of the ADACS subsystem for these two options (CubeSat Kit, 2013). The MAI-400 option is available from Maryland Aerospace (Maryland Aerospace, 2014). The MPACS option is available from Busek (Busek, 2016).

Table 3. Mass and volume of standard ADACS subsystems for CubeSats

ADACS	Mass [g]	Width [mm]	Depth [mm]	Height [mm]	VOLUME [mm^3]	VOLUME [U]
MAI-100	885				810381	0.810381
ADACS	*865*	*100*	*100*	*78.74*	*787400*	*0.7874*
Magnetometer	*20*	*28.7*	*28.7*	*27.9*	*22981*	*0.02298*
MAI-200	930				810381	0.810381
ADACS	*910*	*100*	*100*	*78.74*	*787400*	*0.7874*
Magnetometer	*20*	*28.7*	*28.7*	*27.9*	*22981*	*0.02298*
MAI-400	694	100	100	55.9	559000	0.559
MPACS	500				310000	0.31

The data in Table 3 were averaged to develop distributions for the mass and volume of the ADACS subsystem. Again, the standard deviation was set such that about 95% of the distribution fell between the minimum and maximum cutoffs. The volume of the ADACS subsystem was modeled as a truncated normal distribution, shown in Figure 4, with average 622,440 mm^3, standard deviation 110,000 mm^3, minimum cutoff of 310,000 mm^3, and maximum cutoff of 810,381 mm^3.

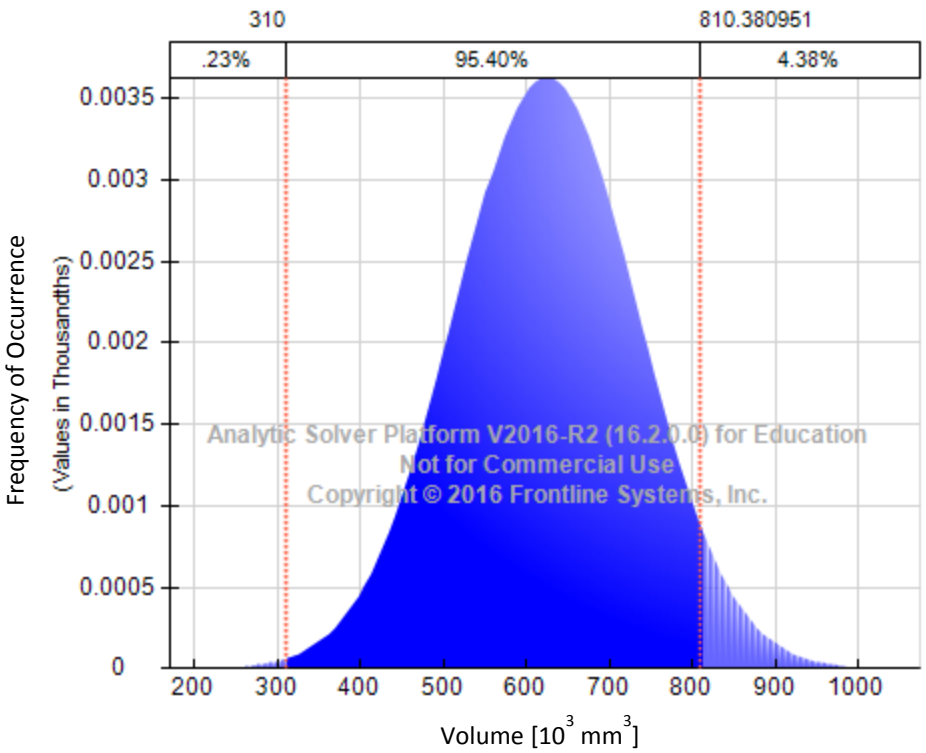

Figure 4. Distribution modeling volume of a CubeSat ADACS subsystem

The mass of the ADACS subsystem was modeled as a truncated normal distribution with mean 0.752 kg, standard deviation 0.1 kg, minimum cutoff of 0.5 kg, and maximum cutoff of 0.93 kg, as shown in Figure 5.

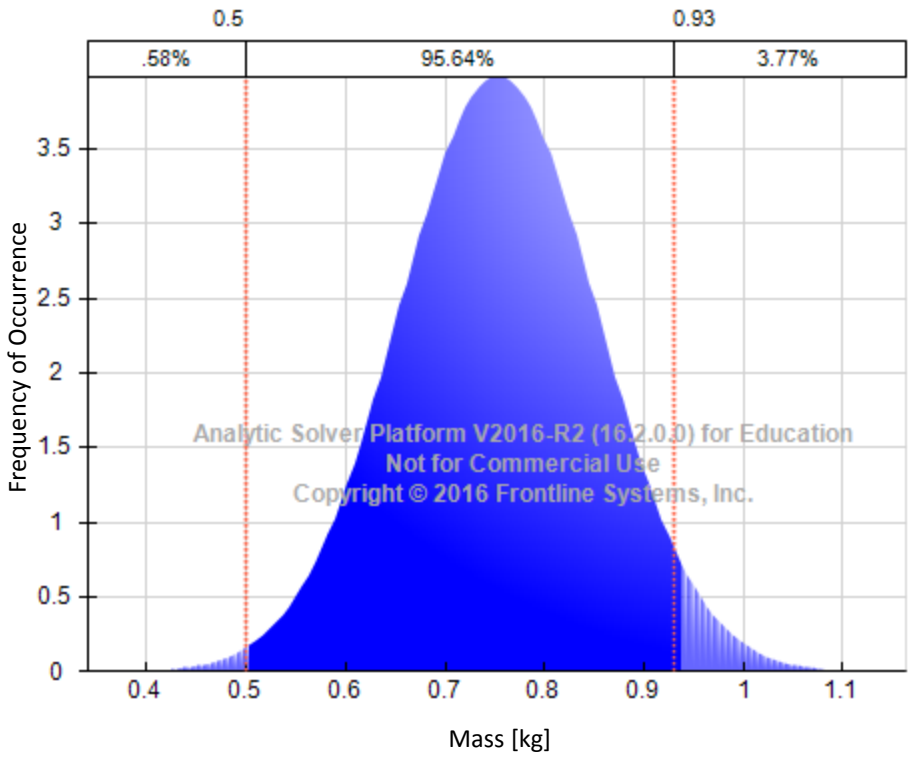

Figure 5. Distribution modeling mass of a CubeSat ADACS subsystem

Propulsion Delta V Modeling

The ΔV data for the propulsion analysis were taken from standard CubeSat propulsion systems from Vacco and are shown in Table 4 (Vacco, 2012). Not all of the systems specified a ΔV; for those that did not, the propellant mass was first estimated using R134-a (liquid density 1225.5 kg/m^3) as the propellant and the volume of the propulsion system as the approximate volume of the propellant. Since the specifications that did include ΔV did so for a 3kg satellite, this was taken as the total mass of the satellite, including the propellant, for the ΔV estimates. These estimates were then used to determine the system's ΔV using Equation 1, a form of the rocket equation.

$$\Delta V = I_{sp} g_0 \ln\left(\frac{M_0}{M_f}\right)$$

Equation 1

Where:

I_{sp} is the specific impulse of the propulsion system,

g_0 is the gravitational constant at the surface of the Earth (or 9.81 m/s^2),

M_0 is the initial mass of the satellite, including propellant (or wet mass), and

M_f is the final mass of the satellite when the propellant has been expended (or dry mass).

The color coding in Table 4 also indicates which of the data were taken directly from the manufacturer's specification and which were estimated.

Table 4. Delta V data and estimates for standard CubeSat propulsion systems

	Volume [U]	delta V [m/s] (3 kg)	Specific Impulse (IsP) [s]	3 kg Spacecraft Dry Mass [kg]	Propellant Mass [g]	Total mass [g]
PUC	0.25	64	-	-	-	-
PUC	0.5	121	-	-	-	-
PUC	1	234	-	-	-	-
MiPS	0.3	51	40	2.63	368	542
MiPS	0.5	90	40	2.39	613	743
MiPS	0.8	155	40	2.02	980	1044
MiPS	1	206	40	1.77	1226	1245
C-POD	1	206	40	1.77	1226	1244

	Specification
	Calculated

The data in Table 4 were plotted and a line fit to the data, as shown in Figure 6.

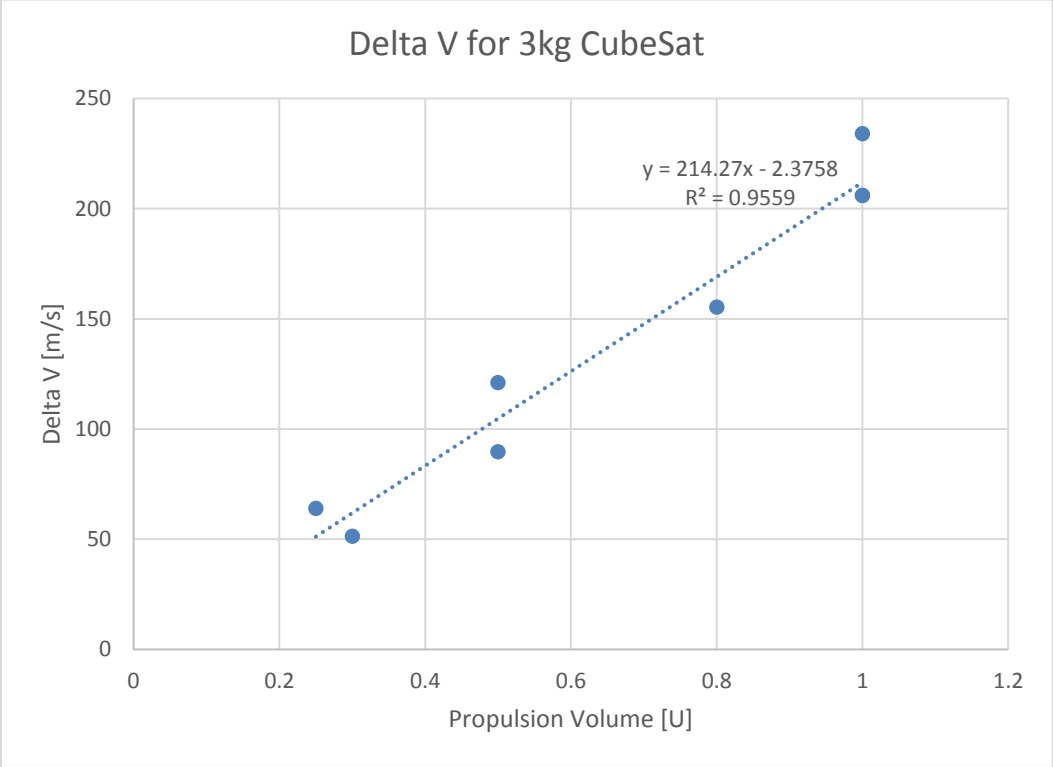

Figure 6. Delta V for standard CubeSat propulsion systems of varying volumes

Equation 2 describes the line fit to the data in Figure 6.

$$y = 214.27x - 2.3758,$$

Equation 2

Where

x is the volume of the propulsion subsystem in U and

y is the ΔV of the propulsion subsystem in m/s, as taken from the manufacturer's spreadsheet or estimated from Equation 1.

The coefficient of determination, or R^2, shows how much the dependent variable can predict the independent variable in a linear fit. The R^2 value of Equation 2 is 0.9559, which indicates that the volume accounts for 95.59% of the correlation. The slope of Equation 2 indicates that according to this model an increase of 1U unit of volume will result in a 214.27 m/s increase in the system's ΔV.

Data for the 3D printed RAMPART CubeSat, which included a 3D printed propulsion design, are shown below in Table 5.

Table 5. Delta V for RAMPART printed CubeSat propulsion design

	Volume [U]	delta V [m/s] (3 kg)	Specific Impulse (IsP) [s]	3 kg Spacecraft Dry Mass [kg]	Propellant Mass [g]
RAMPART design	1	197	90	2.4	600

	Specification
	Calculated

The RAMPART data were used along with the slope from Equation 2 to develop a model predicting ΔV with respect to the volume of a 3D printed propulsion system, detailed in Equation 3.

$$y_{3D} = 214.27x_{3D} - 17.27$$

Equation 3

Where

x_{3D} is the volume in U of the 3D printed propulsion system and

y_{3D} is the predicted ΔV in m/s.

Radiation Hardening Attenuation Modeling

Radiation attenuation is the amount of radiation that is attenuated, or decreased, by traveling through a medium such as radiation shielding. Radiation attenuation is a percentage value and is calculated using Equation 4.

$$1-\frac{I}{I_0}=1-e^{\left(-\mu/\rho t\right)}$$

Equation 4

Where

I is the amount of radiation that is transmitted through the medium,

I_0 is the initial amount of radiation,

μ/ρ is the mass attenuation coefficient, and

t is the thickness of the medium.

The mass attenuation coefficient varies according to material and with the energy of the radiation. The National Institute of Standards and Technology (NIST) has data for the mass attenuation coefficients for various materials available on their website (NIST, n.d.).

For a two-material composite material such as the AM material and tungsten panels described in Kwas and in Shemelya, the radiation attenuation can be calculated using Equation 5 (Shemelya 2015).

$$1-\frac{I}{I_0}=1-e^{-\left(x_1\mu_1/\rho_1+x_2\mu_1/\rho_1\right)\left(x_1\rho_1+x_2\rho_2\right)t}$$

Equation 5

Where

x_1 is the mass fraction of one material in a two-material composite and

x_2 is the mass fraction of the other material in a two-material composite.

Summary

This chapter has summarized the BEAM CubeSat architecture and described how the proposed benefits of that architecture will be assessed against quantitative measures. In addition, this chapter developed quantitative statistical models based on CubeSat kit and component manufacturers' data in the areas of CubeSat mass and volume, electronics mass and volume, ADACS thruster mass and volume, propulsion subsystem delta V and volume, and structural panel radiation attenuation and mass. The following chapter will show the completed BEAM CubeSat architecture and the results of the predictive models presented here.

IV. Analysis and Results

Chapter Overview

This chapter compares the system definition and functional allocation between the AM-augmented BEAM CubeSat architecture and a baseline CubeSat architecture. The architecture views selected in the methodology to represent the mapping between potential benefits, affected subsystems, and measures for the BEAM CubeSat are presented. It then goes on to examine the proposed benefits of additive manufacturing in each of the three areas of embedded electronics, thrusters, and radiation shielding. For each proposed benefit, the measures are identified according to the architecture mapping, and the results of the predictive models developed in the previous chapter are presented and discussed.

Architecture

Most of the views for the BEAM CubeSat architecture emphasize mapping between services, operational activities, systems, and measures for the three previously identified areas of interest and their proposed benefits. However, it is helpful to initially examine the systems interface description (SV-1) and systems functionality description (SV-4) views of a standard CubeSat architecture to define the CubeSat subsystems and their functional allocations without additive manufacturing. These views will provide a baseline for comparison to the SV-1 and SV-4 views of the BEAM CubeSat architecture. The baseline SV-1 in Figure 7 defines and groups the CubeSat subsystems as identified in the literature review.

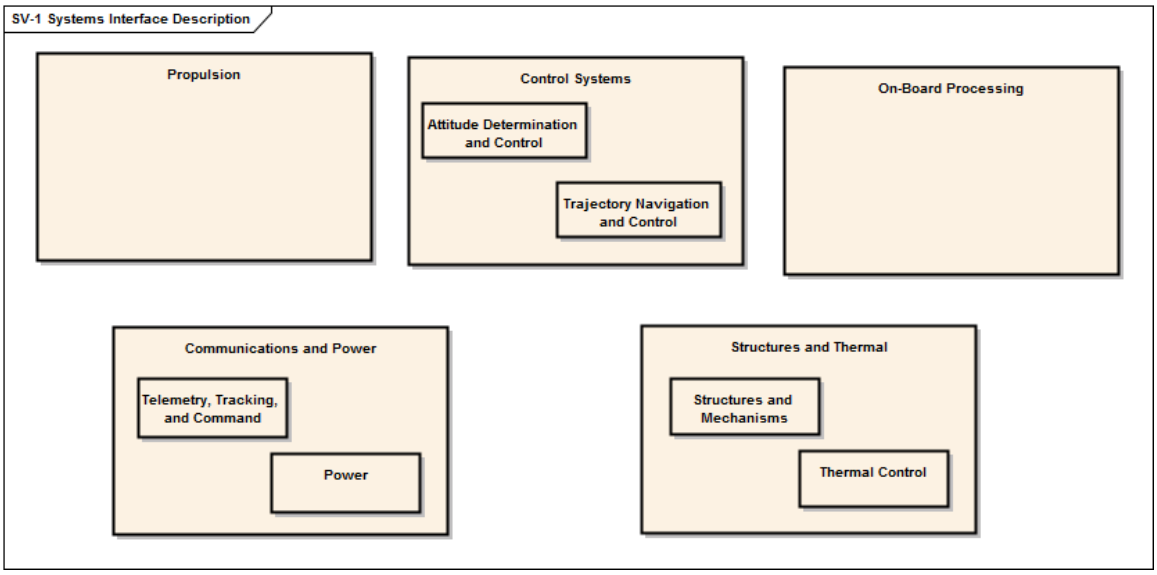

Figure 7. Baseline SV-1: Systems Interface Description

The subsystems from Figure 7 are then used in the baseline SV-4 shown in Table 6 to allocate satellite functions to those subsystems. The satellite functions used in the baseline architecture are based on Stryker's work (Stryker, 2010).

Table 6. Baseline SV-4: Systems Functionality Description

MODULE	Propulsion	ADACS	TNC	On-Board Processing	TT&C	Power	Structures	Thermal Control
FUNCTION								
Sense Attitude								
Control Attitude								
Sense Temperature								
Control Temperature								
Sense Translational Path								
Control Translational Path								
Track Ground Signal								
Import Ground Signal								
Process Ground Signal								
Perform ΔVCommand								
House Spacecraft & Payload Modules								
Protect Spacecraft & Payload Modules								
Provide Electrical Power								
Store Electrical Power								
Distribute Electrical Power								

Figure 7 and Table 6 establish a baseline CubeSat architecture for comparison to the BEAM CubeSat architecture. The BEAM architecture begins with an operational

activity model (OV-5a) in Figure 8 which shows the operational activities involved in 3D printing a CubeSat, including the three AM techniques of interest and their potential impacts. These activities are presented as the first view of BEAM because they define how AM can impact the manufacture of a CubeSat.

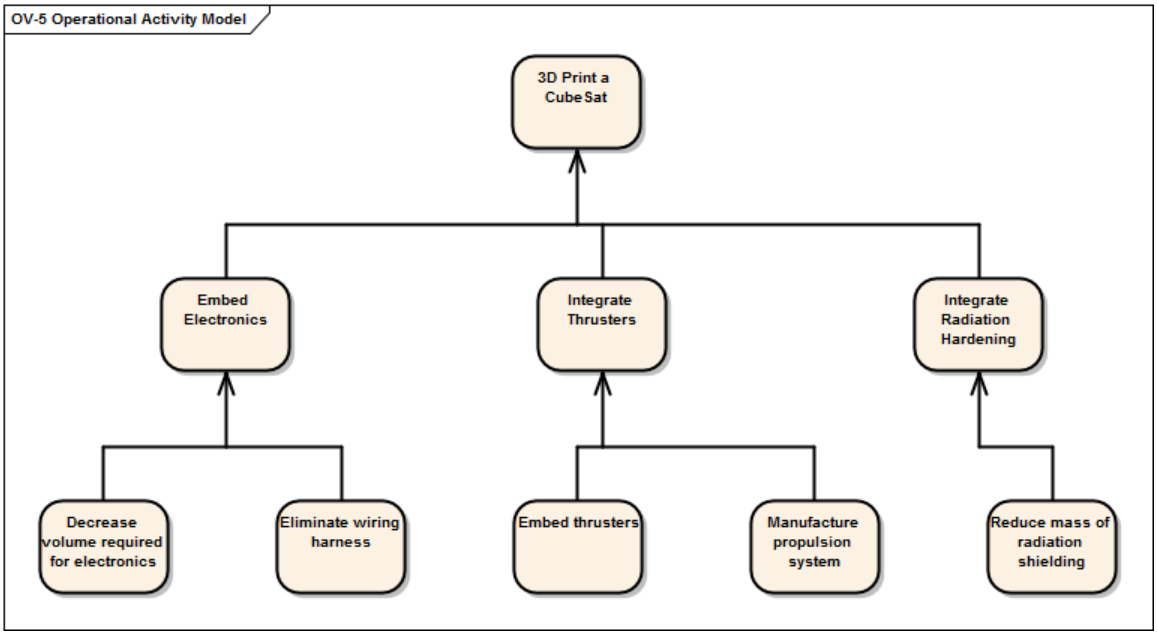

Figure 8. BEAM OV-5a: Operational Activity Model

The operational activities of embedding electronics and integrating thrusters changes the systems interface description of Figure 7. Embedding electronics into the CubeSat structure results in the power subsystem becoming a part of the structures subsystem, rather than part of the communications and power group. This leaves TT&C as a standalone subsystem. Similarly, integrating thrusters by either embedding them in the structure or manufacturing the propulsion system concurrently with the structure results in the previously standalone propulsion subsystem also becoming a part of the structures subsystem. These changes are shown in the AM-augmented BEAM systems interface description in Figure 9.

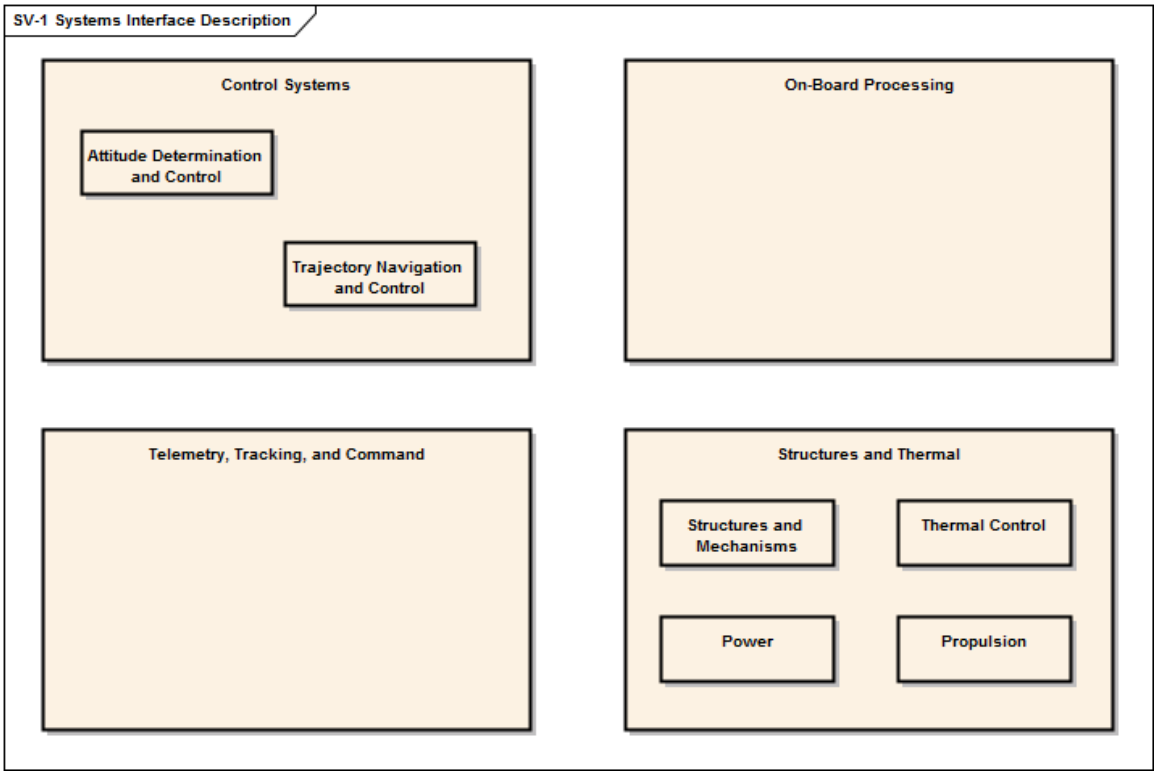

Figure 9. BEAM SV-1: Systems Interface Description

The change in the systems interface from the baseline case to the AM-augmented BEAM case also results in changes to the functional allocations in the BEAM SV-4, as shown in Table 7. As a result of integrating the power and the propulsion subsystems directly into the structure, the CubeSat functions previously allocated to those separate subsystems are now allocated to the structure subsystem. This functional reallocation makes the structures subsystem responsible for the majority of the CubeSat's functions. This integrated as opposed to modular approach could be concerning for a larger satellite, but is less so for a small, relatively inexpensive CubeSat. If there is a change to or a failure in the structure subsystem a large number of satellite functions will be impacted; however, the solution is to simply print the structure again. With additive manufacturing, this is a relatively simple and inexpensive process since there are not upfront tooling

costs. Note that unlike embedding electronics and integrating thrusters, integrating radiation hardening does not impact the functional allocation. Additional radiation protection such as layers of MLI are already considered part of the structures subsystem in the baseline case, and so the function "Protect Spacecraft and Payload Modules" remains with the structures subsystem in both the baseline and AM-augmented cases.

Table 7. BEAM SV-4: Systems Functionality Description

MODULE	TNC	ADACS	On-Board Processing	TT&C	Structures	Thermal Control
FUNCTION						
Sense Attitude						
Control Attitude						
Sense Temperature						
Control Temperature						
Sense Translational Path						
Control Translational Path						
Track Ground Signal						
Import Ground Signal						
Process Ground Signal						
Perform ΔVCommand						
House Spacecraft & Payload Modules						
Protect Spacecraft & Payload Modules						
Provide Electrical Power						
Store Electrical Power						
Distribute Electrical Power						

The remaining views of the BEAM CubeSat architecture focus on defining services as the proposed benefits of the AM augmented CubeSat architecture and mapping those benefits to the BEAM operational activities, subsystems, and measures for the quantitative analysis. The services shown in Figure 10 define the proposed benefits of using AM techniques to develop CubeSats. Enabling a smaller CubeSat to perform the mission and increasing the volume available for the payload relates to the problem statement's need of CubeSat development methods to reduce mass and volume. Decreasing the time spent in integration relates to the problem statement's need for

lowering development cost and schedules, since the hours spent in integration increase both the cost of the satellite and the development time. The ability to change the CubeSat's orbit also helps with lowering development costs, since an increased ability to change to a more desirable orbit post launch increases the number of launch opportunities available to the CubeSat developers.

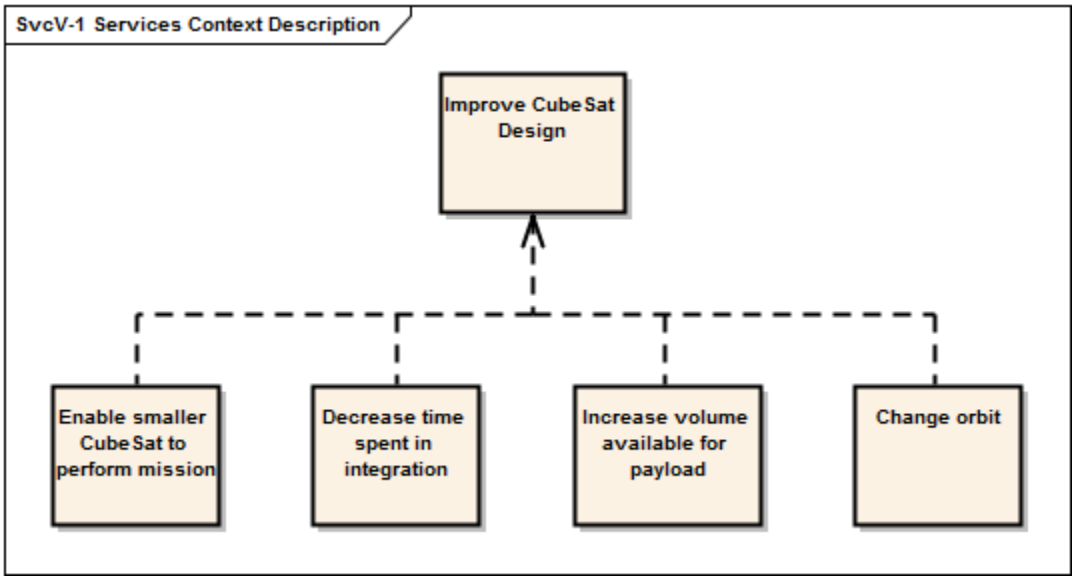

Figure 10. BEAM SvcV-1: Services Context Description

Figure 11 maps the proposed benefits of AM augmented CubeSats to the potential impacts of each AM technique of interest. Embedding thrusters, decreasing the volume required for the electronics, and reducing the mass of the radiation shielding all address the need for lowering a CubeSat's mass and volume. Eliminating the wiring harnesses and printing the propulsion system address the need for lowering development cost and schedule, since they decrease the time spent in integration and increase the CubeSat's ability to change orbit, respectively.

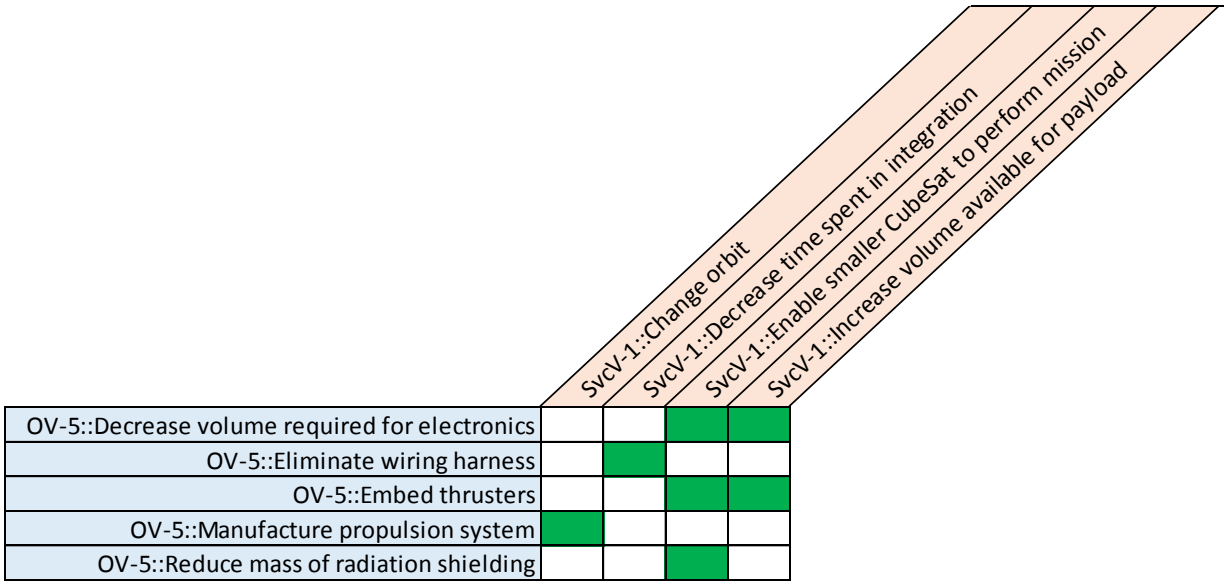

Figure 11. BEAM SvcV-5: Services to Activity Mapping

Figure 12 maps the proposed benefits of using AM techniques to manufacture CubeSats to the CubeSat subsystems as defined in the BEAM SV-1. Not surprisingly, since the power and propulsion subsystems were subsumed by the structures subsystem in the AM-augmented architecture, the structures subsystem is mapped to all four proposed benefits. The services of enabling a smaller CubeSat to perform the mission and increasing the volume available for the payload are also mapped to the control systems because small embedded thrusters can be used to replace larger magnetometers and torque rods as part of the ADACS subsystem.

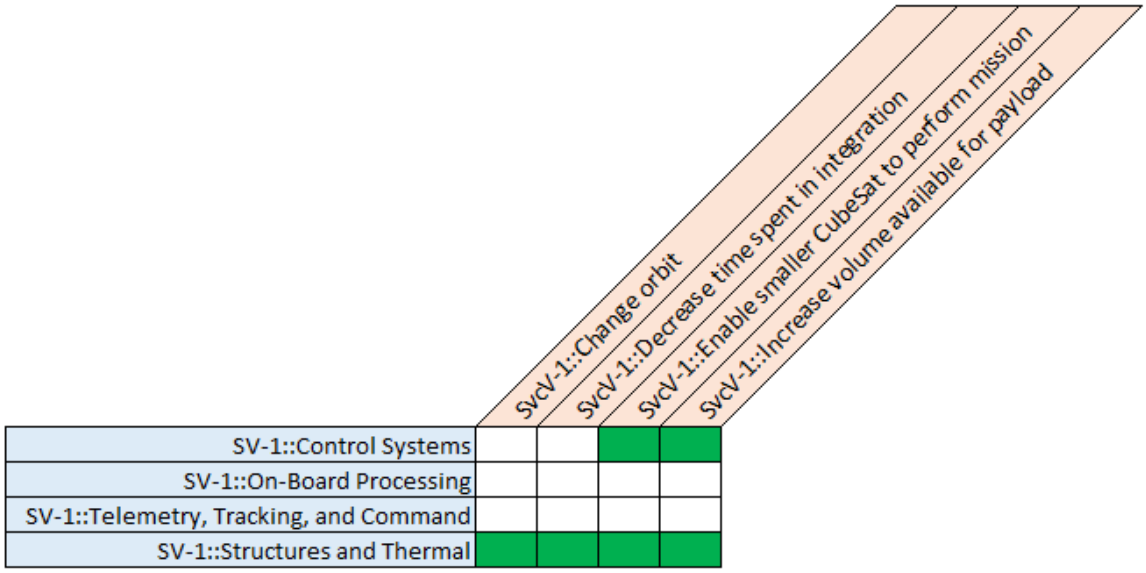

Figure 12. BEAM SvcV-3a: Services to System Mapping

Finally, Figure 13 maps the proposed benefits of 3D printed satellites to the measures used to quantitatively analyze the impact of using AM techniques to manufacture CubeSats. Volume and mass are used to quantify whether a smaller CubeSat can perform the mission and also how much the available payload volume has changed. Delta V is used to quantify how much a CubeSat can change its orbit, and the schedule is used to quantify the impact on the time spent in integration.

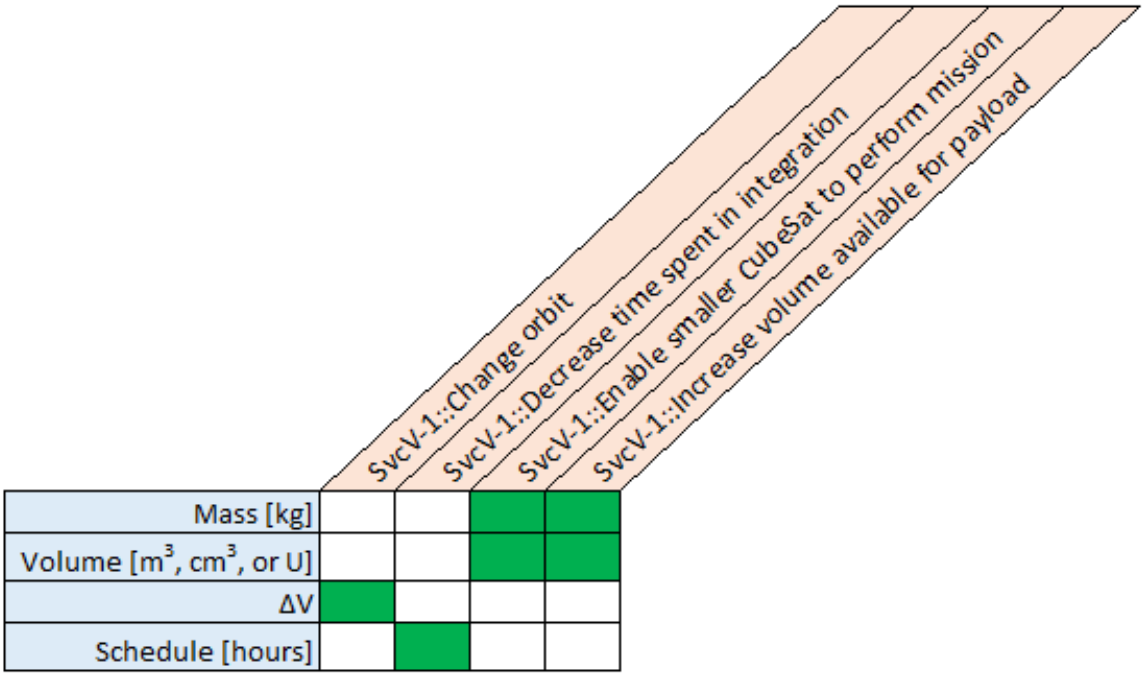

Figure 13. BEAM SvcV-7: Services to Measures Mapping

Integration Time

Because each CubeSat is a unique build, there is no standard amount of time spent in assembly and integration. Unlike hardware subsystems where data sheets are readily available from the manufacturers, a quantitative analysis of the assembly and integration phase would require data from each individual satellite build, which is not readily accessible within the scope of this work. However, an examination of a typical satellite assembly, integration, and test process flow can at least qualitatively address the impact of AM techniques on this phase of the development cycle and even give some insight into the magnitude of that impact. Figure 14 shows a simplified process flow for the assembly, integration, and test of a standard satellite (Stryker, 2010). The major phases of the process are bus assembly and test, payload assembly and test, and spacecraft integration and test.

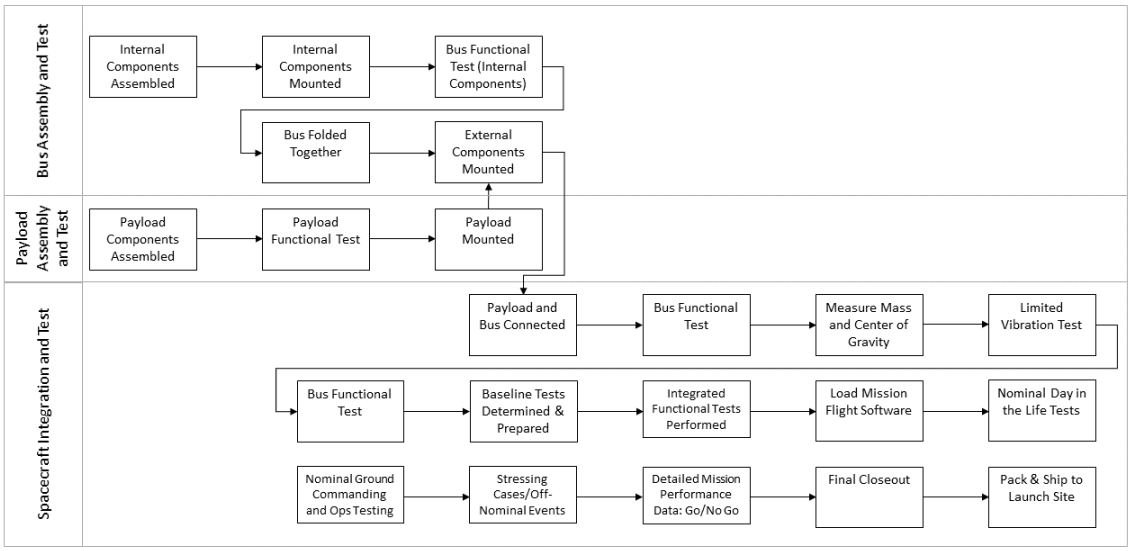

Figure 14. CubeSat Assembly, Integration, and Test Process Flow

Figure 15 shows how using AM techniques to manufacture key components of the CubeSat impacts this process. An AM-augmented CubeSat fabrication process eliminates two and decreases time spent in two of the twenty-two total steps.

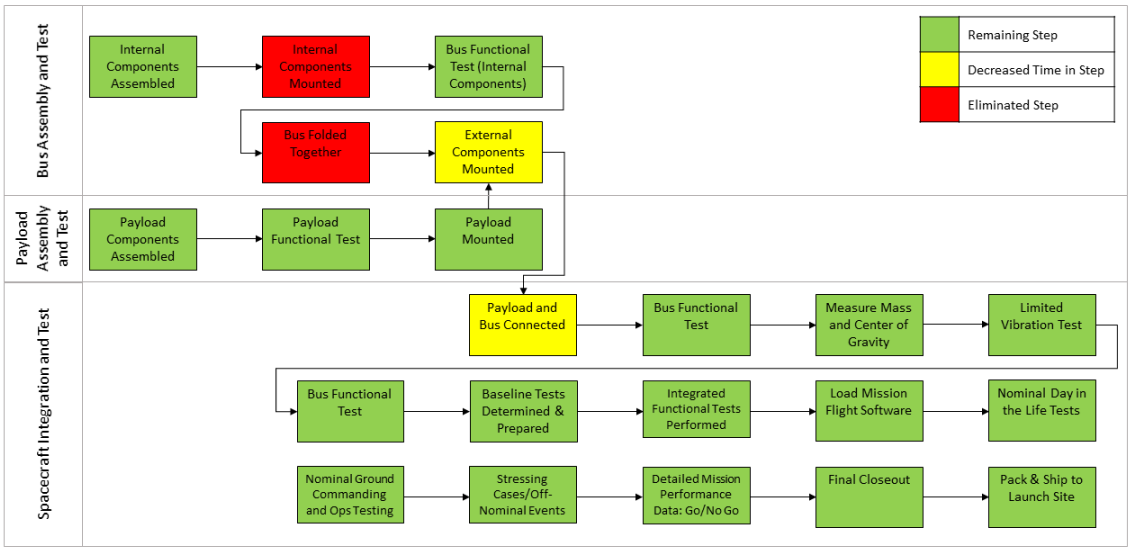

Figure 15. AM-Augmented CubeSat Assembly, Integration, and Test Process Flow

Most of the impact of the AM techniques occur in the bus assembly and test phase. Because the internal components of the CubeSat bus such as electronics and any thrusters or propulsion systems are already embedded during the fabrication of the bus structure, the step of mounting these components to the bus structure is eliminated. However, because these components are embedded and not necessarily directly printed—for example, a small thruster can be embedded in the structure with AM techniques without the thruster itself being printed—it is necessary to maintain the step of assembling the internal components prior to embedding. In addition, there is no need to fold the bus together, since the bus has been printed as a single structure with the internal bus components already embedded in the structure.

Because each payload is unique, this work does not consider the impact of printing or embedding the payload itself, and so the AM techniques presented here do not

affect the payload assembly and test phase. However, it is reasonable to assume that embedding the power subsystem directly into the spacecraft structure would reduce the complexity of wiring harnesses, and thus reduce the time required to connect the bus and payload. This step is the only step in the spacecraft integration and test phase impacted by the AM techniques presented in this work since the remainder of the phase focuses on developing and executing tests on the fully integrated CubeSat. Although it is outside the scope of this work, it is worth noting any advances towards making the AM techniques presented here a space qualified process could reduce the number of tests required during this phase and the bus assembly and test phase, thus decreasing the non-recurring costs of space qualification.

Embedded Electronics

Benefit 1

The first proposed benefit of using AM techniques to embed electronics directly into the satellite structure is enabling a smaller CubeSat to perform the mission by decreasing volume required for electronics. The measures for this benefit are volume in 1U units and mass. Units of 1U are used for the analysis of this benefit since a smaller satellite can only be used if volume savings are in increments of 1U—for example, if embedded electronics reduce a 3U satellite's volume to 2.5U, a 3U satellite must still be used for the mission to be compatible with the standardized CubeSat dispenser.

Chapter 3 described in detail the statistical volume and mass models for the electronics subsystem and for various sizes of CubeSat. These models were then used to predict the volume and mass of the CubeSat with decreasing size of the electronics

subsystem. Figure 16 shows the predicted volume of CubeSats ranging in size from 1U to 6U if AM embedding decreases the volume of the electronics subsystem by 10% through 90%. The plot shows a decrease in absolute volume that is constant across all sizes of CubeSat, which is to be expected since it was assumed in the electronics subsystem model that all sizes of CubeSat used the same size of electronics subsystem. The maximum volume decrease shown is 0.82U caused by a 90% electronics subsystem volume decrease.

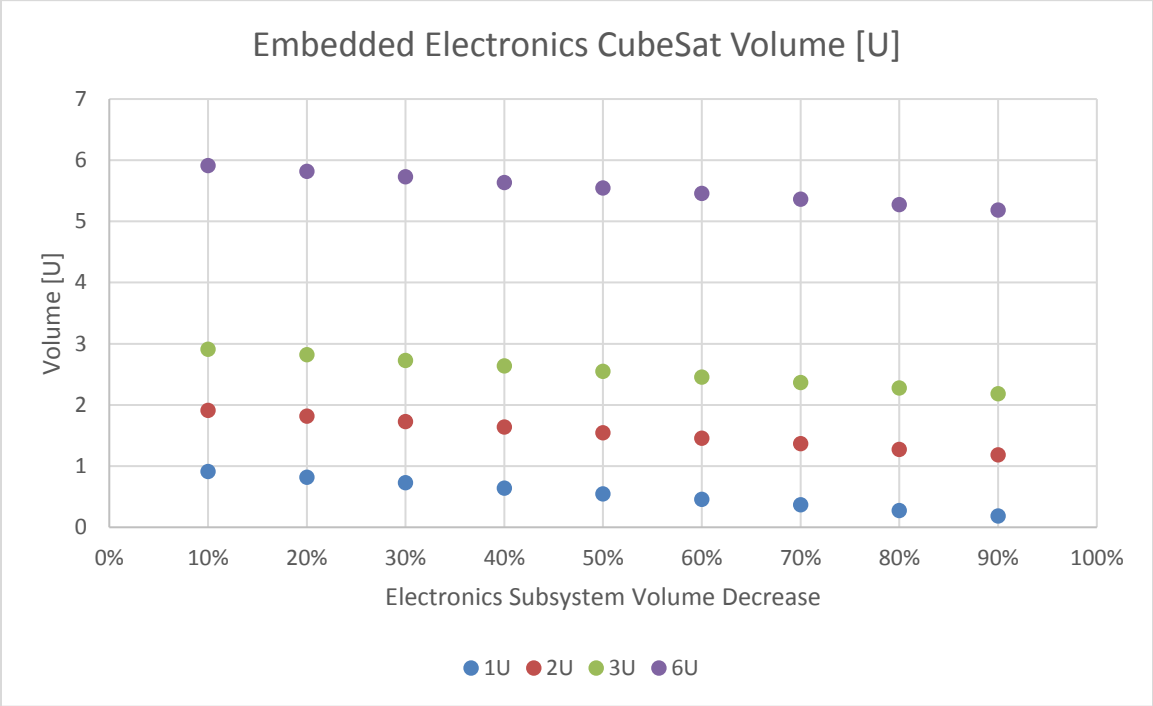

Figure 16. Predicted volume [U] of CubeSat with embedded electronics

The same results are also shown in Table 8 to illustrate whether the volume decrease is enough to enable the use of a smaller standard CubeSat size. As can be seen from the table, only the 2U size can be decreased to another standard CubeSat size—a 60% to 90% decrease in the volume of the electronics subsystem would be enough to enable the use of a 1.5U CubeSat. All other standard CubeSat sizes, however, are in units

of whole U, and since none of the other sizes result in the decrease of an entire U, embedded electronics alone would not be enough to enable use of a smaller standard volume CubeSat.

Table 8. Average volume [U] of CubeSat with embedded electronics

	Average Volume [U]				
Decrease	*1U*	*2U*	*3U*	*6U*	+/-
10%	0.90	1.90	2.90	5.90	0.005
20%	0.82	1.82	2.82	5.82	0.010
30%	0.73	1.73	2.73	5.73	0.016
40%	0.64	1.64	2.64	5.64	0.021
50%	0.55	1.55	2.55	5.55	0.026
60%	0.46	1.46	2.46	5.46	0.031
70%	0.36	1.36	2.36	5.36	0.037
80%	0.27	1.27	2.27	5.27	0.042
90%	0.18	1.18	2.18	5.18	0.047

Figure 17 shows the predicted mass percent decrease with respect to decreasing electronics subsystem mass. Decreasing the electronics subsystem has the largest impact on the 1U CubeSat, and minimal impact on the 6U CubeSat.

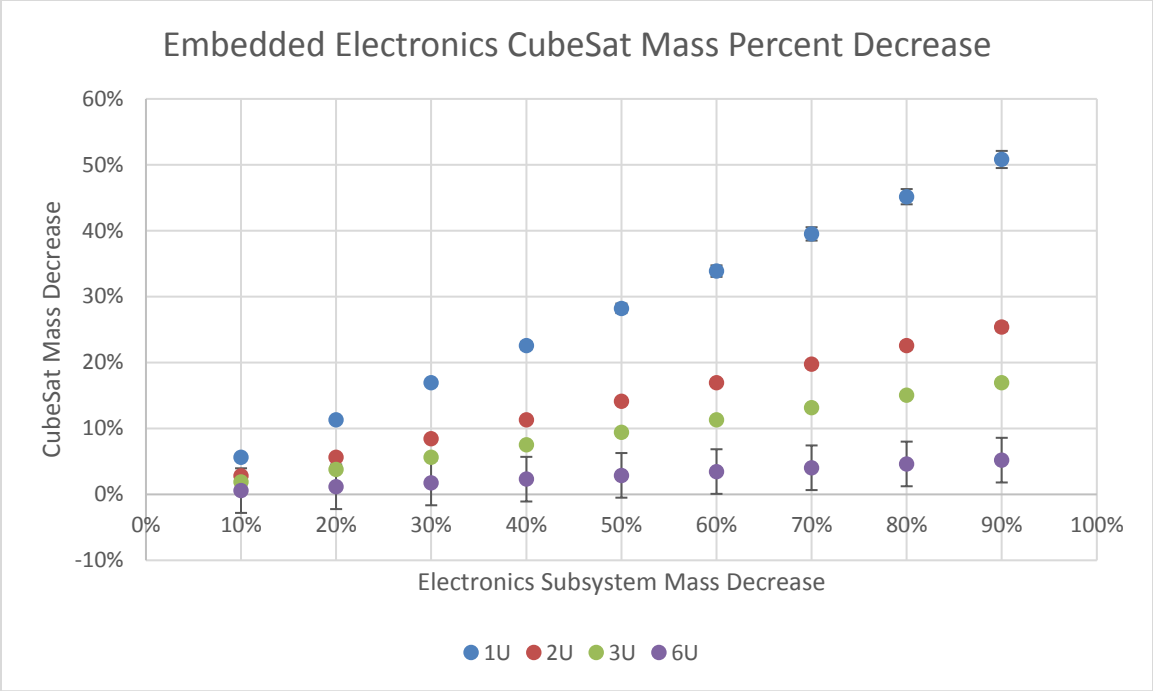

Figure 17. Predicted mass percent decrease of CubeSat with embedded electronics

Benefit 2

The second proposed benefit of using AM techniques to embed electronics directly into the satellite structure is increasing the volume available for the payload by decreasing the volume required by electronics. The measures for this benefit are again volume and mass, so this analysis uses the models for electronics subsystem and CubeSat volumes and masses previously developed in Chapter 3. Although the volume and mass savings could be used in a variety of ways, such as adding extra fuel, this work focuses on how much more payload could be added instead. Focusing on the amount the payload can change instead of adding fuel allows for factors such as ΔV to remain constant throughout the analysis.

Figure 18 shows the available payload volume increase as a percentage of the total satellite volume for 1U through 6U satellites as the volume of the electronics

subsystem is decreased via embedded electronics. Again, the largest impact is on the 1U satellite, which demonstrates a 9.08 ± 0.52% increase in volume available for payload at just a 10% decrease in the volume of the electronics subsystem and up to an 81.71 ± 4.69% increase with a 90% decrease in the volume of the electronics subsystem. The least impact is on the 6U CubeSat, which is predicted to have just a 1.51 ± 0.09% increase in available payload volume at a 10% decrease in the volume of the electronics subsystem, and a 13.62 ± 0.78% increase at a 90% decrease in the volume of the electronics subsystem.

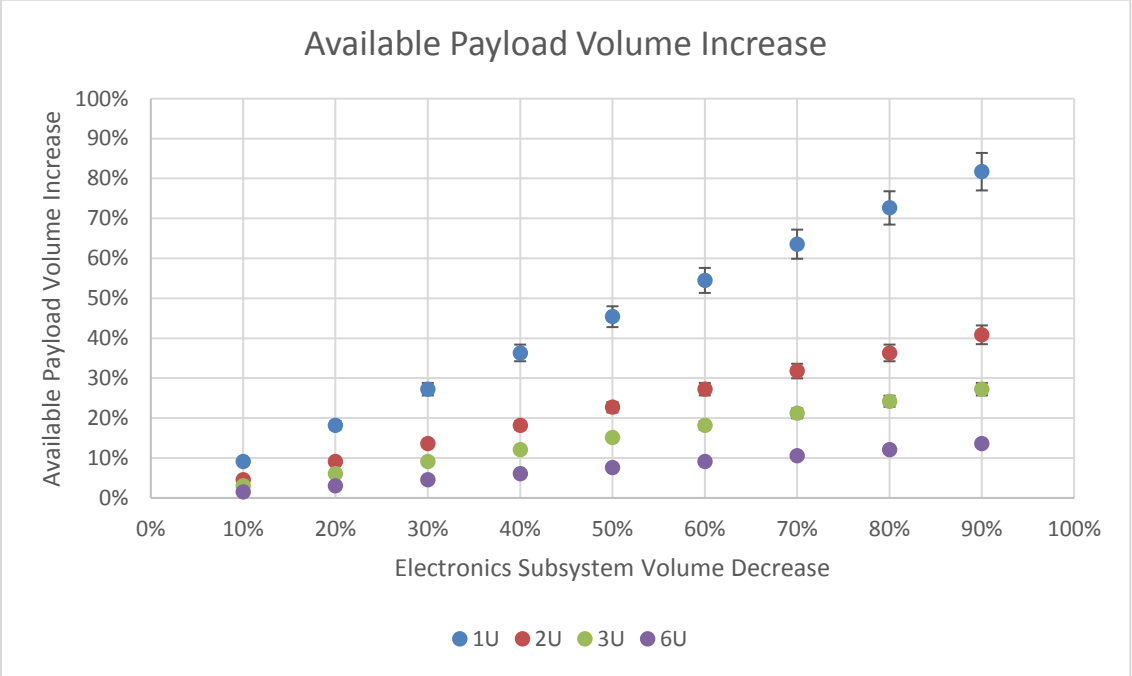

Figure 18. Available payload volume increase with embedded electronics

Figure 19 shows the predicted increase in mass budget available for the payload as the mass of the electronics subsystem decreases with embedded electronics for CubeSats ranging from 1U to 6U. A 1U, 2U, or 3U satellite will have between 0.075 ± 0.002 kg and 0.676 ± 0.017 kg available in the mass budget for additional payload. A 6U

CubeSat differs only in standard deviation, having between 0.075 ± 0.440 kg and 0.676 ± 0.440 kg available in the mass budget for additional payload.

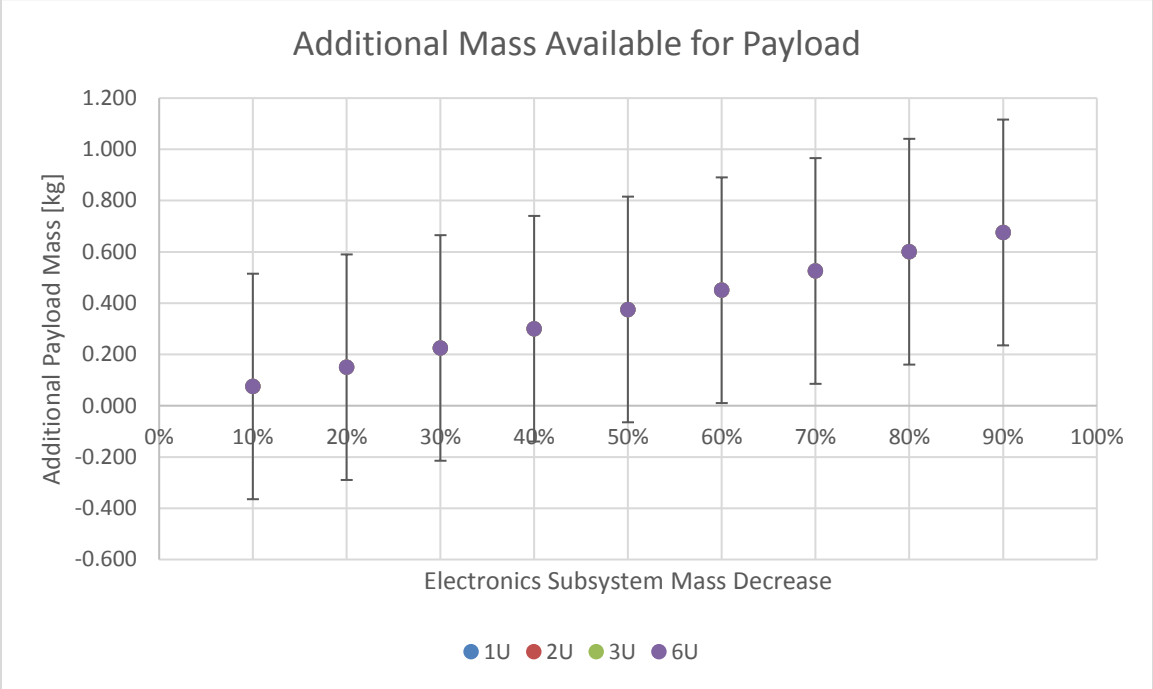

Figure 19. Available payload mass increase with embedded electronics

Thrusters

Benefit 1

Another proposed benefit of using AM techniques to embed thrusters is enabling a smaller CubeSat to perform the mission by embedding thrusters to reduce the volume and mass required for ADACS. The measures for this benefit are volume and mass. This analysis uses the models for a CubeSat and the ADACS subsystem masses and volumes developed in Chapter 3.

Figure 20 shows the predicted volume decrease of a CubeSat with respect to decrease in ADACS volume due to embedded thrusters.

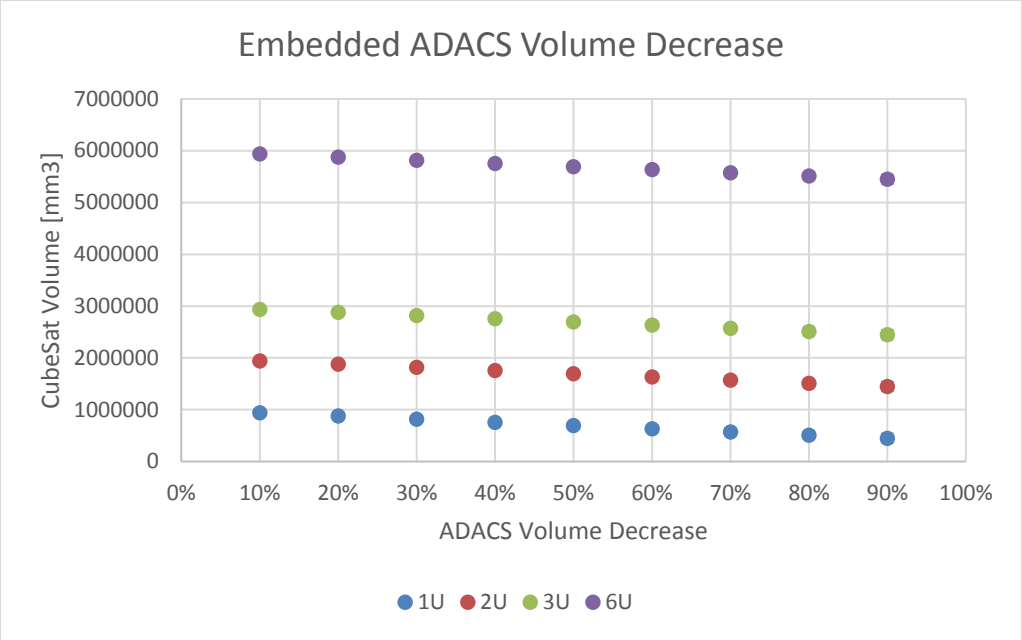

Figure 20. Predicted volume decrease with embedded ADACS

Figure 21 shows the predicted mass decrease of a CubeSat with respect to decrease in ADACS mass due to embedded thrusters. The plot shows a constant decrease across all sizes of CubeSat, which is reasonable since it was assumed that the ADACS subsystem is the same regardless of CubeSat size. Because of this, the largest impact in terms of percent total mass is on the 1U CubeSat.

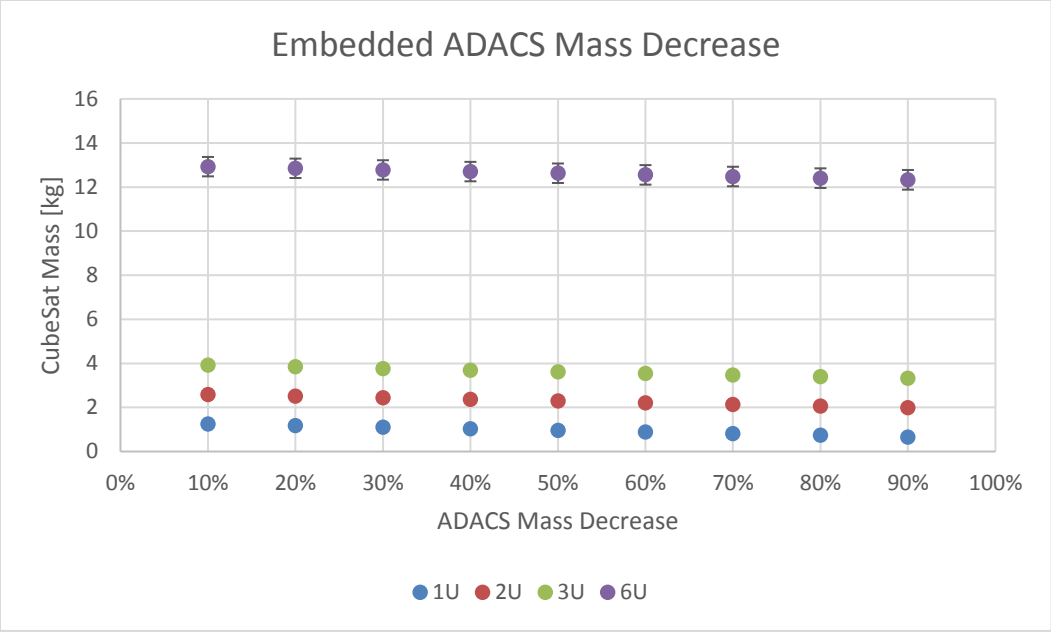

Figure 21. Predicted mass decrease with embedded ADACS

Benefit 2

Another proposed benefit of a 3D printed satellite is the ability to enable a secondary-payload-CubeSat to change orbit by building new small propulsion designs with AM techniques. The measure for this benefit is delta V (ΔV) in meters per second. This analysis uses the propulsion delta V model developed in Chapter 3.

Recall that Equation 3 from Chapter 3 used the RAMPART data along with the slope of the correlation between ΔV and volume for standard CubeSat propulsion systems to predict ΔV with respect to the volume of a 3D printed propulsion system. This predictive model of Equation 3 is shown plotted in Figure 22, indicating that that 3D printed propulsion systems provide less ΔV for the same propulsion subsystem volume. According to this model the ΔV per 1U volume of printed propulsion subsystem is predicted to be 71% (for 0.25 U propulsion subsystems) to 93% (for 1U propulsion subsystems) of the ΔV per 1U volume of a current standard CubeSat propulsion

subsystem. This decrease indicates that, for now at least, 3D printed propulsion systems require a slightly larger volume to achieve the same ΔV as standard CubeSat propulsion systems.

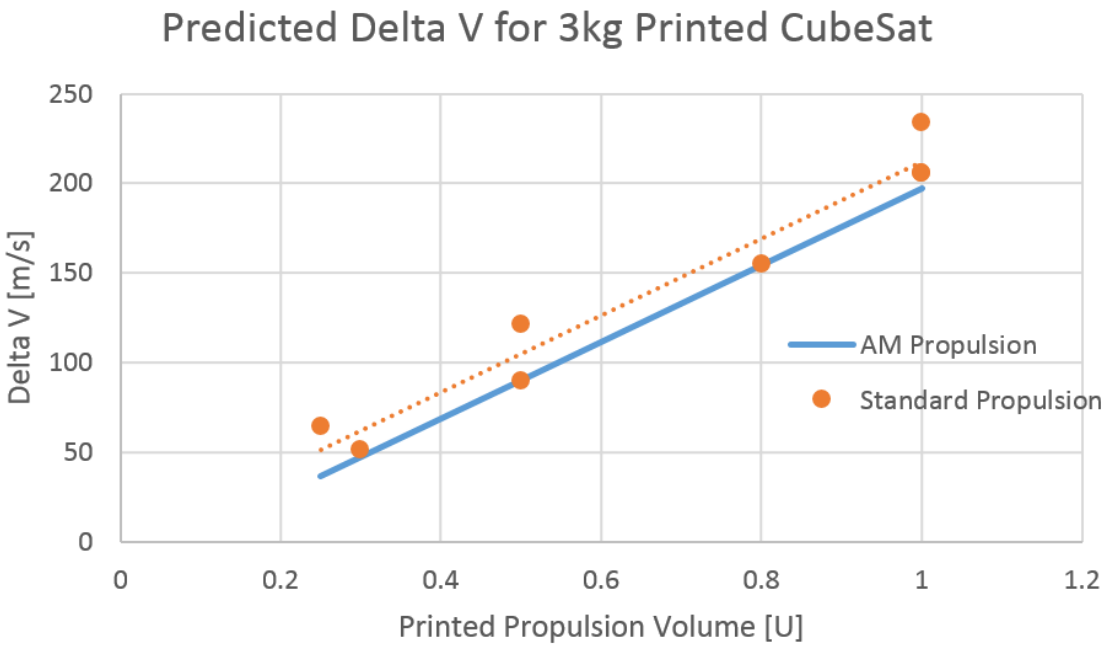

Figure 22. Predicted delta V for printed propulsion systems of varying volumes

Radiation Hardened Materials

Benefit 1

The last potential benefit of 3D printed satellites examined in this work is the ability to enable a lighter CubeSat to perform the mission by printing the satellite from radiation hardened materials. The measure for this benefit is mass for the same or better radiation attenuation performance as modeled in Equation 4 and Equation 5 of Chapter 3.

This analysis compares standard CubeSat shielding structures of 0.127" thickness made from the current choice of aluminum and from the 95% AM material and 5%

tungsten composite described in Shemelya (Shemelya 2015). Polymethyl methacrylate (PMMA) was chosen as the AM material since it was the closest material to the one described in Shemelya with mass attenuation coefficient data readily available from NIST. Mass attenuation coefficient data for aluminum, PMMA, and tungsten was taken from NIST, and used in Equation 4 and Equation 5 to model the radiation attenuation of the CubeSat shielding structure made from aluminum and that made from a PMMA-tungsten composite, respectively. The predicted attenuation of the CubeSat panel from 40 to 150 KeV (the approximate range tested in Shemelya) is shown in Figure 23.

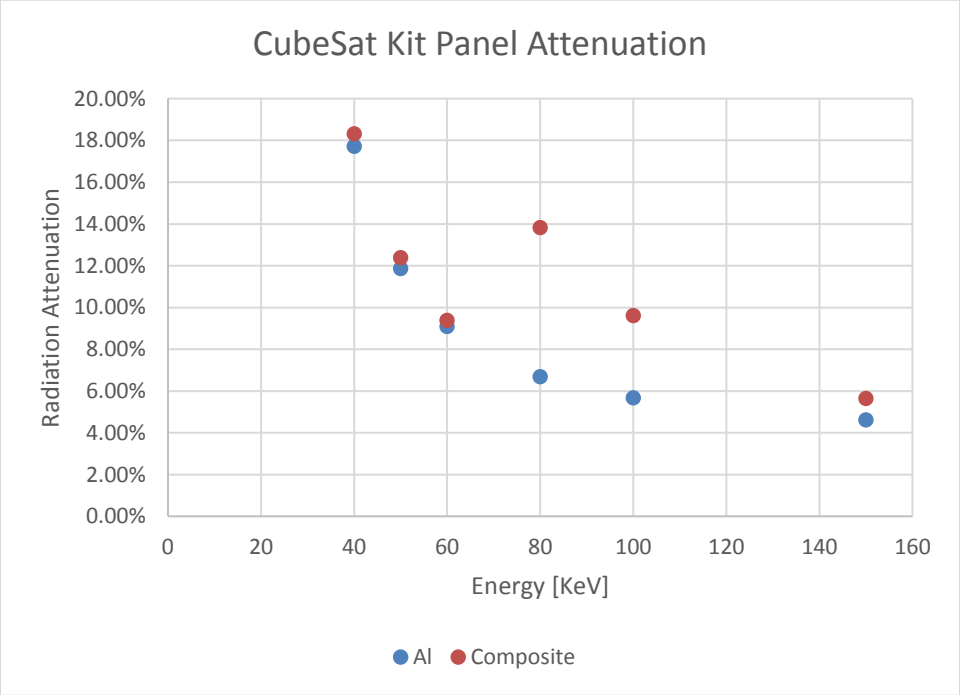

Figure 23. Predicted radiation attenuation of aluminum and AM composite CubeSat kit panel

Figure 23 shows that the AM composite panel performs the same or better than the standard aluminum panel, depending on the energy of the radiation—at 80 KeV, the composite provides over twice the attenuation as the standard aluminum panel! Using

the satellite mass model discussed in previous sections for 1U, 2U, 3U, and 6U CubeSats, it was estimated that replacing the aluminum CubeSat panels with a PMMA-tungsten composite material could reduce the mass of the radiation shielding panels by 22% across all four CubeSat sizes studied, as shown in Table 9. This decreases the mass of the overall satellite by up to 3% for a 1U CubeSat and 1% for a 6U CubeSat.

Table 9. Mass decrease using AM composite panels vs. aluminum shielding panels

Satellite Volume [U]	% Mass Decrease of Radiation Shielding	Total Satellite % Mass Savings
1	22%	3%
2	22%	3%
3	22%	3%
6	22%	1%

Summary

This chapter presented a simple architecture for a CubeSat built with additive manufacturing techniques and compared the system definitions and functional allocations of this architecture to those of a baseline CubeSat architecture. The proposed benefits were mapped to subsystems and measures within the BEAM architecture and quantitatively evaluated against those measures using the predictive models developed in Chapter 3. The quantitative analysis determined that the BEAM architecture would result in decreased mass and volume, increased ΔV, and increased radiation attenuation with decreased mass for a custom PMMA-Tungsten material. Although the results held for CubeSats of all sizes, only the radiation attenuation had the same percent increase and mass percent decrease for CubeSats of all sizes. Mass and volume decreases and ΔV

increases had the maximum impact on 1U CubeSats and the least impact on 6U CubeSats.

V. Conclusions and Recommendations

Introduction of Research

To address the issues of long development schedules and high development and manufacturing costs, methods are needed in the CubeSat development process to reduce the weight and volume of subsystems and decrease integration time. Proponents of additive manufacturing technology propose many potential benefits related to weight, volume, and taking an integrated instead of modular approach to CubeSat manufacturing. This study focused on three main proposed benefits of AM technology: embedding electronics and other components to optimize mass and volume, enabling the manufacture of propulsion and ADACS that rely on AM's ability to produce unique geometries, and embedding components in custom materials to increase radiation protection. The research developed a CubeSat architecture enhanced by these AM techniques and developed predictive models based on current data from CubeSat manufacturers to quantitatively address what impact the architecture would have on the subsystems of a CubeSat.

Summary of Research Gap, Research Questions, and Answers

The objective of this research was to bridge the gap between proposed benefits of AM technology and the needs of CubeSat developers through the development and analysis of quantitative models based on current CubeSat data. To meet this objective the research focused on answering three investigative questions.

The first investigative question addressed what an AM-augmented CubeSat architecture would look like. To answer the question, this study developed the BEAM

CubeSat architecture, an architecture for a CubeSat with key components built using AM techniques. The BEAM architecture was compared to a standard CubeSat architecture as a baseline. The comparison determined that an AM-augmented CubeSat architecture would have a different grouping of subsystems, since integrating electronics and propulsion into the satellite's structure would make the power and propulsion subsystems part of the larger structure subsystem instead of acting as standalone subsystems. Because of this change, the functions of the power and propulsion subsystems were reallocated from the standalone subsystems in the baseline architecture to the structure subsystem in the BEAM architecture. This functional reallocation highlighted the difference between a traditional modular CubeSat approach and a new AM-led integrated approach, since most of the satellite's functions were now allocated to the single large structures subsystem.

The second investigative question addressed on which CubeSat subsystem the AM-augmented architecture would have the greatest impact. The BEAM architecture comparison indicated that AM techniques would have the greatest impact on the structures subsystem. Again, embedding electronics and thrusters into the satellite's structure means that the structure subsystem subsumes the power and propulsion subsystems, making the structure subsystem responsible for the bulk of the CubeSat's functions.

The third and final investigative question asked which of the three main benefits of AM techniques under study—embedding electronics, embedding thrusters, and radiation hardening—would have the greatest impact on an AM-augmented CubeSat. The results of the quantitative analysis indicate that enhancing radiation hardening with

custom 3D-printed materials would provide the most impact. Replacing standard aluminum CubeSat structural panels with a PMMA-tungsten composite material could reduce the mass of the panels by 22% while increasing the radiation attenuation by up to double that of the standard aluminum panel, depending on the radiation's energy level. This conclusion held across the 1U, 2U, 3U, and 6U sizes studied, unlike the results for embedded electronics and thrusters, which showed the maximum impact for the smallest, 1U size.

Study Limitations

This study assumed that the technology already exists to manufacture key components of a satellite with AM techniques. The previous and current research presented in the literature review suggests that this assumption is feasible in perhaps a ten to twenty year timeframe due to the optimization and space qualification necessary to produce flight hardware. In addition, the data used to build the models were limited to that available from CubeSat kit and component manufacturers, which limited the ability of this study to quantify the impact of AM techniques on the length of time spent during the assembly, integration, and testing phase. Any recommendations on whether the Air Force should take action to invest in AM methods for building CubeSats is also outside the scope of this work.

Recommendations for Future Research

Some of the idealized assumptions, such as the electronics subsystem and the ADACS components staying the same size across all sizes of CubeSat, were used to

simplify the modeling. A future approach could include taking into account how the size of these subsystems varies with the size of the CubeSat.

One interesting approach to continuing this work could begin with developing a database of all CubeSat launches to date, including approximations for overall development time and time spent in the various development phases as well as concrete mass, volume, and delta V budgets. This database could then be used to develop more rigorous statistical and predictive models for the type of analysis and results presented in this work. Such a database would also address the previously mentioned limitations of the integration and testing time analysis as well as any simplifying assumptions regarding how size of subsystems varies with the size of the CubeSat.

Summary

This work indicates that using an AM-augmented architecture to build CubeSats changes the manufacturing process from a traditional modular approach to an integrated approach, with the bulk of a CubeSat's functions residing not in the interior of the satellite but directly inside the structure. In addition, this research suggests that although there are a number of benefits in the area of reducing mass and volume through unusual geometries, perhaps the most productive area of AM research for space applications is in the arena of custom materials for radiation hardening. AM provides a unique opportunity to produce custom materials, such as the PMMA-tungsten composite discussed here, with relative ease and inexpense compared to traditional manufacturing. Combined with the integrated build approach also enabled by AM, embedding the bulk of a satellite's functions inside a custom material with improved radiation hardening could be a game-

changing technology for CubeSat manufacturers. It is the author's hope that this research will contribute to a larger discussion on the role of additive manufacturing in improving the development and manufacturing processes for space-based technologies.

Bibliography

Gutierrez, Cassie, et al. "CubeSat Fabrication through Additive Manufacturing and Micro-Dispensing." *Proceedings from the IMAPS Symposium.* 2011.

Medina, Frank, et al. "Hybrid Manufacturing: Integrating Direct-Write and Stereolithography." *Proceedings of the 2005 Solid Freeform Fabrication Symposium.* 2005.

Lopes, A.J., et al. "Expanding rapid prototyping for electronic systems integration of arbitrary form." *Proceedings of the 17th Annual Solid Freeform Fabrication Symposium, University of Texas at Austin, Austin, TX*. Society of Manufacturing Engineers, 2006.

Navarrete, Misael, et al. *Integrated layered manufacturing of a novel wireless motion sensor system with GPS.* Texas University at El Paso W.M. Keck Center for 3D Innovation, 2007.

Perez, K.B., Williams, C.B., "Combining Additive Manufacturing and Direct Write for Integrated Electronics—A Review." *Solid Freeform Fabrication Symposium, University of Texas at Austin, Austin, TX.* 2013.

Swartwout, Michael. "The first one hundred cubesats: A statistical look." *Journal of Small Satellites* 2.2 (2013): 213-233.

Marshall, William M., et al. "Using Additive Manufacturing to Print a CubeSat Propulsion System." *51st AIAA/SAE/ASEE Joint Propulsion Conference*. 2015.

Moore, Gilbert, et al. "3D Printing and MEMS Propulsion for the RAMPART 2U CUBESAT." (2010).

Kwas, Andrew, et al. "Enabling Technologies for Entrepreneurial Opportunities in 3D printing of SmallSats." (2014).

Wertz, James Richard, David F. Everett, and Jeffery John Puschell, eds. *Space Mission Engineering: The New SMAD*. Microcosm Press, 2011.

Shemelya, Corey, et al. "Mechanical, Electromagnetic, and X-ray Shielding Characterization of a 3D printable Tungsten-Polycarbonate Polymer Matrix Composite for Space-Based Applications." *Journal of Electronic Materials*, 2015.

CubeSat Kit. (2013). http://www.cubesatkit.com. Accessed 14 May 2016.

Thompson, Tabatha. “NASA Opens New CubeSat Opportunities for Low-Cost Space Exploration.” (2015). http://www.nasa.gov/press-release/nasa-opens-new-cubesat-opportunities-for-low-cost-space-exploration. Accessed 14 May 2016.

Maryland Aerospace. (2014). http://d6110363.ozt807.onezerotech.com/products/s/mai-400/. Accessed 22 May 2016.

Busek. (2016). http://www.busek.com/. Accessed 22 May 2016.

Vacco. (2012). http://www.cubesat-propulsion.com/vacco-systems/. Accessed 22 May 2016.

NIST. (n.d.). http://physics.nist.gov/PhysRefData/XrayMassCoef/tab3.html. Accessed 27 May 2016.

Stryker, Amie C. “Development of Measures to Assess Product Modularity and Reconfigurability.” AFIT, 2010.

REPORT DOCUMENTATION PAGE

Form Approved
OMB No. 074-0188

1. REPORT DATE *(DD-MM-YYYY)*	**2. REPORT TYPE**	**3. DATES COVERED** *(From – To)*
15-09-2016	Master's Thesis	January 2016 – September 2016

TITLE AND SUBTITLE

Evaluation of the Impact of an Additive Manufacturing Enhanced CubeSat Architecture on the CubeSat Development Process

5a. CONTRACT NUMBER

5b. GRANT NUMBER

5c. PROGRAM ELEMENT NUMBER

6. AUTHOR(S)

Sharples, Rachel E., Civilian, Ctr

5d. PROJECT NUMBER

5e. TASK NUMBER

5f. WORK UNIT NUMBER

7. PERFORMING ORGANIZATION NAMES(S) AND ADDRESS(S)
Air Force Institute of Technology
Graduate School of Engineering and Management (AFIT/EN)
2950 Hobson Way, Building 640
WPAFB OH 45433-7765

8. PERFORMING ORGANIZATION REPORT NUMBER

AFIT-ENV-MS-16-S-049

9. SPONSORING/MONITORING AGENCY NAME(S) AND ADDRESS(ES)

Intentionally left blank

10. SPONSOR/MONITOR'S ACRONYM(S)

11. SPONSOR/MONITOR'S REPORT NUMBER(S)

12. DISTRIBUTION/AVAILABILITY STATEMENT
DISTRUBTION STATEMENT A. APPROVED FOR PUBLIC RELEASE; DISTRIBUTION UNLIMITED.

13. SUPPLEMENTARY NOTES
This material is declared a work of the U.S. Government and is not subject to copyright protection in the United States.

14. ABSTRACT
Additive manufacturing (AM) is a fabrication method ideally suited to low-quantity, highly customized builds, leading to interest in its application to satellite development and manufacturing, where each build is unique. Due to the issues of long development schedules and high development and manufacturing costs, methods are needed in the CubeSat development process to reduce the weight and volume of subsystems and decrease integration time. The work develops an architecture for an AM-augmented CubeSat and examines the AM techniques of embedded electronics, embedded thrusters, and custom radiation-hardened materials can impact the subsystems of a CubeSat. The AM-augmented architecture shows a shift in CubeSat development and manufacturing from a modular approach to an integrated approach where most of the CubeSat's internal bus components, such as electronics, thrusters, and propulsion, are integrated directly into the structure. This integrated approach results in decreased time spent in assembly and integration, decreased mass and volume, and also allows for key components to be embedded in materials with improved radiation attenuation characteristics.

15. SUBJECT TERMS
Additive manufacturing, CubeSat, architecture

16. SECURITY CLASSIFICATION OF:			**17. LIMITATION OF ABSTRACT**	**18. NUMBER OF PAGES**	**19a. NAME OF RESPONSIBLE PERSON**
a. REPORT	**b. ABSTRACT**	**c. THIS PAGE**			Lt Col Jeffrey Parr, AFIT/ENV
U	U	U	UU	89	**19b. TELEPHONE NUMBER** (937) 255-3636, x4709 jeffrey.parr@afit.edu

Standard Form 298 (Rev. 8-98)
Prescribed by ANSI Std. Z39-18